

Sensory and Motor Systems

Heterozygous *Dcc* Mutant Mice Have a Subtle Locomotor Phenotype

Louise Thiry,^{1,*} Chloé Lemaire,^{1,*} Ali Rastqar,^{1,*} Maxime Lemieux,^{1,*} Jimmy Peng,^{2,3,*} Julien Ferent,^{2,3} Marie Roussel,¹ Eric Beaumont,⁴ James P. Fawcett,^{5,6}  Robert M. Brownstone,⁷  Frédéric Charron,^{2,3,8,†} and  Frédéric Bretzner^{1,9,†}

<https://doi.org/10.1523/ENEURO.0216-18.2021>

¹Centre de Recherche du Centre Hospitalier Universitaire (CHU) de Québec-Université Laval, Centre Hospitalier de l'Université Laval (CHUL)–Neurosciences P09800, Quebec City, Quebec G1V 4G2, Canada, ²Institut de Recherches Cliniques de Montréal (IRCM), Montréal, Quebec H2W 1R7, Canada, ³Department of Biology, McGill University, Montréal, Quebec H3G 0B1, Canada, ⁴Department of Biomedical Sciences, Quillen College of Medicine, East Tennessee State University, Johnson City, TN 37604, ⁵Department of Pharmacology, Dalhousie University, Halifax, Nova Scotia B3H 4R2, Canada, ⁶Department of Surgery, Dalhousie University, Halifax, Nova Scotia B3H 4R2, Canada, ⁷University College London (UCL) Queen Square Institute of Neurology, University College London, London WC1N 3BG, United Kingdom, ⁸Department of Medicine, University of Montreal, Montréal, Quebec H3C 3J7, Canada, and ⁹Department of Psychiatry and Neurosciences, Université Laval, Quebec City, Quebec G1V 4G2, Canada

Abstract

Axon guidance receptors such as deleted in colorectal cancer (DCC) contribute to the normal formation of neural circuits, and their mutations can be associated with neural defects. In humans, heterozygous mutations in *DCC* have been linked to congenital mirror movements, which are involuntary movements on one side of the body that mirror voluntary movements of the opposite side. In mice, obvious hopping phenotypes have been reported for bi-allelic *Dcc* mutations, while heterozygous mutants have not been closely examined. We hypothesized that a detailed characterization of *Dcc* heterozygous mice may reveal impaired corticospinal and spinal functions. Anterograde tracing of the *Dcc*^{+/-} motor cortex revealed a normally projecting corticospinal tract, intracortical microstimulation (ICMS) evoked normal contralateral motor responses, and behavioral tests showed normal skilled forelimb coordination. Gait analyses also showed a normal locomotor pattern and rhythm in adult *Dcc*^{+/-} mice during treadmill locomotion, except for a decreased occurrence of out-of-phase walk and an increased duty cycle of the stance phase at slow walking speed. Neonatal isolated *Dcc*^{+/-} spinal cords had normal left-right and flexor-extensor coupling, along with normal locomotor pattern and rhythm, except for an increase in the flexor-related motoneuronal output. Although *Dcc*^{+/-} mice do not exhibit any obvious bilateral impairments like those in humans, they exhibit subtle motor deficits during neonatal and adult locomotion.

Key words: CPG; *Dcc*; locomotion; mutant mice

Significance Statement

We show that loss of one deleted in colorectal cancer (*Dcc*) allele does not affect motor cortex, corticospinal efficacy, or skilled locomotor control in adult mice, but it increases flexor-related motoneuronal output in the developing spinal cord and increases duty cycle of the stance phase during treadmill locomotion at slow walking speeds in adult mice. This finding raises the possibility of the existence of subtle locomotor changes in humans carrying monoallelic *DCC* mutations.

Received May 31, 2018; accepted December 20, 2021; First published February 3, 2022.

The authors declare no competing financial interests.

Author contributions: R.M.B., J.P.F., F.C., and F.B. designed research; L.T., C.L., A.R., M.L., J.P., M.R., J.F., E.B., and F.B. performed research; L.T., C.L., A.R., M.L., J.P., M.R., J.F., E.B., F.C., and F.B. analyzed data; L.T., C.L., M.L., J.P., F.C., and F.B. wrote the paper.

Introduction

Individuals carrying monoallelic deleted in colorectal cancer (*DCC*) mutations exhibit congenital mirror movements, which are unintentional movements on one side of the body that are mirror reversals of intended unilateral movements on the opposite side (Schott and Wyke, 1981; Srour et al., 2010). Bilateral motor responses can be evoked in response to unilateral transcranial magnetic stimulation of the motor cortex in these people (Srour et al., 2010; Welniarz et al., 2017) and, these bilateral motor responses are correlated with an abnormal bilateral projection of their corticospinal fibers at the level of the pyramidal decussation (Welniarz et al., 2017). This phenotype in *DCC* heterozygous humans is most likely a result of haplo-insufficiency, given that many of the mutations are predicted to result in mRNA degradation or truncated *DCC* proteins (Izzi and Charron, 2011; Peng and Charron, 2013). The receptor *DCC* mediates a chemoattractive signal to Netrin-1 (Keino-Masu et al., 1996; Fazeli et al., 1997; Jain et al., 2014; Srivatsa et al., 2014), thereby contributing to the normal development of a wide variety of axonal tracts, including those of spinal commissural interneurons (Rabe Bernhardt et al., 2012) and corticospinal tracts (Finger et al., 2002). Mutations in *NETRIN-1* also cause mirror movements in human (Méneret et al., 2017). Loss of floor plate Netrin-1 in mice impairs midline crossing of corticospinal and spinal axons and leads to a bilateral forelimb movement phenotype reminiscent of human mirror movements (Pourchet et al., 2021).

In contrast to *DCC*^{+/-} humans, heterozygous *Dcc*^{+/-} mice exhibit no overt mirror-like phenotypes. Bi-allelic *Dcc* null mutant mice die at birth, precluding the possibility of studying their motor cortex and corticospinal tract projection through adulthood (Fazeli et al., 1997). However, mutant mice carrying the bi-allelic *kanga* mutation (*Dcc*^{kanga/kanga}), a spontaneous mutation that removes the P3 intracellular domain, are viable and exhibit an abnormal rabbit-like hopping gait (Finger et al., 2002). The hopping gait phenotype is different from the bilateral forelimb movement phenotype: while the former is mostly known to occur because of axon crossing defects in spinal interneurons (Kullander et al., 2003; Talpalar et al.,

2013; Peng et al., 2018), the latter has been linked to crossing defects of the corticospinal tract (Serradj et al., 2014; Pourchet et al., 2021). Corticospinal tract lateralization defects produce phenotypes more akin to the mirror-movement phenotype observed in *DCC*^{+/-} humans.

DCC and its ligand Netrin-1 are also important for normal development of sensory afferents to the dorsal spinal cord (Ding et al., 2005; Watanabe et al., 2006) and spinal commissural interneurons (Keino-Masu et al., 1996; Fazeli et al., 1997; Rabe et al., 2009; Rabe Bernhardt et al., 2012; Dominici et al., 2017; Varadarajan et al., 2017). Spinal cords isolated from neonatal wild-type (WT) mice produce spontaneous left-right alternating neuronal activity on bath application of neurotransmitters, which reflect the output of the locomotor central pattern generator (Jiang et al., 1999; Thiry et al., 2016). Interestingly, neonatal *Netrin-1* mutant spinal cords exhibit a reduction in the number of commissural interneurons including V0 commissural interneurons, whereas V3 commissural interneurons are spared and presumably contribute to the synchronization of left and right locomotor activities (Rabe Bernhardt et al., 2012). However, both neonatal *Dcc*^{-/-} and *Dcc*^{kanga/kanga} spinal cords exhibit a robust reduction in the number of most commissural interneurons, including V0 and V3 commissural interneurons, thus leading to disorganization of the coupling between left and right locomotor activities (Rabe Bernhardt et al., 2012). More recently, it has been shown that a selective *Dcc* mutation in spinal interneurons (*HoxB8*^{cre}; *Dcc*^{flox/-} and *HoxB8*^{cre}; *Dcc*^{flox/flox}) exhibits a robust hopping phenotype in adult mice (Peng et al., 2018), indicating that local spinal cord defects following loss of *Dcc* cause a hopping gait. Given the strong phenotype reported in various neonatal and adult biallelic *Dcc* mutant spinal cords, we hypothesized that a heterozygous *Dcc* mutation might be sufficient to result in a neuroanatomical, neurophysiological, and motor phenotype, aiding in our understanding of the impairment of motor control seen in people carrying monoallelic *DCC* mutations.

Using axonal tract tracing, intracortical microstimulation (ICMS), and behavioral tests, we found that pyramidal decussation was normal, as was corticospinal efficacy in producing responses in forelimb and hindlimb muscles of adult *Dcc*^{+/-} mice, with no obvious functional impairments in their skilled motor control. Furthermore, no gait and posture dysfunctions were observed during treadmill locomotion, except for a decrease in the occurrence of out-of-phase walk and a longer duty cycle for the stance phase at slow treadmill speed. In spinal cord preparations isolated from neonatal mice, spinal interneuronal circuits exhibited normal locomotor pattern and rhythm; nevertheless, the flexor-related motoneuronal output was significantly increased in neonatal *Dcc*^{+/-} spinal cords. In summary, although *Dcc*^{+/-} mice do not exhibit any obvious bilateral impairments like those in humans, they exhibit subtle motor deficits during neonatal and adult locomotion.

Materials and Methods

All animal procedures were performed in accordance with the Dalhousie University, Institut de Recherches Cliniques de Montréal (IRCM) and Université Laval animal

This work was supported by the Canadian Institutes of Health Research (CIHR) Grant 334023, the Fonds de Recherche du Québec-Santé (FRQS) Grant 27003, and the Canada Foundation for Innovation (CFI) Grant 33768 (to F.C.); CIHR Grants MOP 341174 (to J.P.F.) and 79413 (to R.M.B.); and the Natural Sciences and Engineering Research Council of Canada (NSERC) Grant 2018-06218 (to F.B.). J.P. was supported by a CIHR Vanier Canada Graduate scholarship. J.F. was supported by FRQS and CIHR fellowships. F.C. holds the Canada Research Chair in Developmental Neurobiology. F.B. is a FRQS Chercheur-Boursier (284011).

*L.T., C.L., A.R., M.L. and J.P. contributed equally to this work.

†F.C. and F.B. are co-senior authors.

Acknowledgements: We thank Béatrice Frenette and Josée Seigneur for technical help.

Correspondence should be addressed to Frédéric Charron at frederic.charron@ircm.qc.ca or Frédéric Bretzner at frederic.bretzner.1@ulaval.ca.

<https://doi.org/10.1523/ENEURO.0216-18.2021>

Copyright © 2022 Thiry et al.

This is an open-access article distributed under the terms of the Creative Commons Attribution 4.0 International license, which permits unrestricted use, distribution and reproduction in any medium provided that the original work is properly attributed.

care committee's regulations. *Dcc*^{+/-} mice were previously generated by the insertion of a neomycin resistance cassette into exon three of the *Dcc* gene (Fazeli et al., 1997). Immunoprecipitation experiments demonstrated that no full-length protein was produced from this allele in homozygous mutant mice (Fazeli et al., 1997).

DCC protein level quantification by Western blotting

Spinal cords were dissected at E13.5, similarly to previously published (Langlois et al., 2010). Tissue was lysed with RIPA buffer (50 mM HEPES pH 7.4, 150 mM NaCl, 10% glycerol, 1.5 mM MgCl₂, 1% Triton X-100, 1% SDS, and 1 mM EDTA) with protease inhibitors (Roche 11873580001) and boiled in SDS sample buffer for 5 min. Protein samples were separated by SDS-PAGE and then transferred to PVDF membrane. The membranes were incubated with 5% skim milk in TBST (0.01 M Tris-HCl pH 7.5, 150 mM NaCl, and 0.1% Tween 20) for 1 h at room temperature, followed by primary antibody incubation (goat anti-DCC, 1:400, A-20, Santa Cruz Biotechnology and mouse anti-actin, 1:1000, Sigma, catalog #A5441) in 1% skim milk in TBST, overnight at 4°C. After three washes in TBST, membranes were incubated for 2 h at room temperature, with secondary antibodies, which were conjugated to horseradish peroxidase (anti-goat HRP, 1:10,000, Jackson ImmunoResearch, catalog #705-035-147 and anti-mouse HRP, 1:10,000, Jackson ImmunoResearch, catalog #115-035-003). After three washes in TBST and a final wash in TBS (without Tween 20), Western blottings were visualized with chemiluminescence.

BDA tracing and analysis of the corticospinal tract

Five adult WT and five *Dcc*^{+/-} animals were anesthetized with ketamine/xylazine (100/10 mg/kg body weight) and a hand drill (Dremel) was used to create a small opening in the skull; 5 μ l of biotinylated dextran amine (10% in PBS, Invitrogen, 10,000 MW) was injected unilaterally into the motor cortex with a syringe (Hamilton, 80300) and the animal was sutured and allowed to recover. After 14 d, animals were perfused in 4% paraformaldehyde (PFA) in PBS and the spinal cord and brain were dissected and postfixed in 4% PFA overnight before cryoprotection in 30% sucrose in PBS and freezing of segments in tissue freezing medium (O.C.T. compound); 30- μ m cryosections of brain and spinal cord were incubated in streptavidin-488 (Jackson ImmunoResearch, 1:200 in PBS + 0.1% Triton X-100) for 2 h at room temperature, mounted, and imaged with a Leica DM4000 fluorescent microscope.

ICMS

Mice were anaesthetized with ketamine-xylazine (100/10 mg/kg body weight). When necessary, supplementary doses of ketamine were administered. The cranial bone was drilled to expose the motor cortex (approximate coordinates bregma +2 to -3, lateral 0.5-3). A tungsten electrode (0.1 M Ω) was inserted up to a depth of 0.7-0.8 mm. Cathodal pulses (10-80 μ A, 0.2-ms duration, trains of 30 ms, interval 2.8 ms) were delivered through this

electrode. A silver wire attached to the skin was used as the anode. To evoke motor response in the hindlimb, the electrode was positioned in the hindlimb representation of the motor cortex (about bregma -1 to -2 mm, lateral -1 to -2) in 11 WT mice and 13 *Dcc*^{+/-} mice. In five WT mice and five *Dcc*^{+/-} mice, we stimulated the forelimb caudal areas (bregma 0 to -1, lateral -1 to -2).

Electromyographic (EMG) probes organized in a duplex configuration (Ritter et al., 2014; Lemieux and Bretzner, 2019) were inserted in the tibialis anterior (TA) on both sides. When we stimulated the forelimb caudal area, we inserted EMG probes in the biceps brachialis (BB). For technical reason, we did not attempt to record the ipsilateral BB. The threshold was evaluated to evoke movements of the ankle and/or knee for the hindlimb and the wrist and/or elbow for the forelimb. The threshold was defined as the current intensity evoking movements 50% of the time or more. For EMG recordings, success rates, latencies, and the number of motor spikes were quantified. We analyzed the number of motor spikes rather than the amplitude of motor spikes because the number of spikes is less dependent on the position of electrodes, which makes it a more reliable approximation of the motor response.

Skilled motor and locomotor behaviors

Cylinder test

Unilateral and bilateral forelimb movements were assessed in a glass beaker for the cylinder test, a vertical exploratory test (Bretzner et al., 2008, 2010; Sparling et al., 2015). A mirror was placed behind the cylinder with an angle to have an overall view of the mouse. Mice were videotaped for 20 rightings using a 40-Hz camera. The use of the left, right, or both forelimbs was scored as the first paw contact and the total number of contacts for each righting. To evaluate motor lateralization, the score was expressed as a percentage of use of the left, right, or both forelimbs relative to the total number of first or total forepaw contacts.

Beam locomotion

Motor coordination and balance were assessed while mice crossed a wide (12 mm width) and a narrow (6 mm width) beam of 40 cm long each (Luong et al., 2011; Fleming et al., 2013). After training, mice were videotaped at a sampling frequency of 40 Hz for three crossings. The number of steps, foot-slip errors, and the time to cross the beam were quantified offline from videos. The percentage of foot-slips was computed as the number of foot-slip errors relative of the number of steps for each crossing and was then averaged for three trials per animal.

Horizontal ladder locomotion

Mice were trained to walk on a horizontal ladder with a regular (1 cm spacing) rung arrangement pattern (Metz and Whishaw, 2002; Laflamme et al., 2019). After training, mice were videotaped for three crossings using a 40-Hz camera. Videos were analyzed frame by frame to assess the number of steps, foot-slip errors, and the time to cross the ladder. The percentage of foot-slip errors was

calculated as the number of errors relative of the number of steps for each trial. The number of steps and the percentage of foot-slip errors were averaged for each mouse for the three trials. The percentage of hindpaw slipping was not reported because it happened only when mice fell from the ladder after forepaw slip.

Treadmill locomotion

Eight WT and nine *Dcc*^{+/-} six-month-old mice were placed on a treadmill (Cleversys Systems Inc.) equipped with a transparent belt. The treadmill speed was adjusted at 15, 20, and 30 cm/s. Each mouse performed two 20-s trials at each speed (from lowest to highest) and was allowed a 3-min rest between each trial. All mice were filmed from below the belt with a high-frequency camera (100 frames/s, Basler) and videos were analyzed offline using custom software as previously described (Lemieux et al., 2016). To avoid acceleration and deceleration phases, videos were analyzed during steady-state locomotion. The timing of lifts and contacts for all four limbs were extracted manually and used for step cycle analysis by computing (1) stance duration: the interval between the foot contact with the belt and the subsequent foot lift; (2) swing duration: the interval between the foot lift and the next foot contact; (3) step cycle: the interval between two successive foot contacts in each limb; and (4) stride frequency: the inverse of the step cycle.

Gait analysis during treadmill locomotion

Locomotor gaits were defined by the interlimb coupling between stance phases of four limbs and locomotor frequencies (number of step cycles per second). Using custom-written routines in MATLAB (The MathWorks), gaits of WT and *Dcc*^{+/-} mice were analyzed during treadmill locomotion at 15, 20, and 30 cm/s. As these speeds were low to intermediate, analysis was focused on three gaits: out-of-phase walk, lateral walk, and trot (Lemieux et al., 2016). Two slow walking gaits, pace and diagonal walk, were excluded from the analysis because of their weak occurrence in mice.

Neonatal locomotor-like activity

Spinal cords from WT and *Dcc*^{+/-} mice dissected out on postnatal days 1–3 were used for *in vitro* experiments. Animals were anesthetized by intraperitoneal injection of ketamine/xylazine (100/10 mg/kg), decapitated, and eviscerated. Spinal cords were isolated by vertebrectomy at room temperature in oxygenated (95% O₂, 5% CO₂) artificial CSF (aCSF) containing 127 mM NaCl, 3 mM KCl, 26 mM NaHCO₃, 1.25 mM NaH₂PO₄, 2 mM CaCl₂, 1 mM MgCl₂, and 10 mM glucose. Spinal cords were cut at the thoracic Th10/11 and sacral S2/3 levels and placed ventral side up in a recording chamber superfused with oxygenated aCSF. Left and right lumbar L2 and L5 ventral roots were attached to suction electrodes designed and selected to fit the specific size of each recorded ventral root, thus ensuring a perfect seal of the suction electrode. The spinal cord was then allowed to recover for at least 30 min before electroneurographic (ENG) recording.

Chemically evoked locomotor-like activity was induced by bath application of a cocktail of neurotransmitters: 5-hydroxytryptamine (5HT; 10 μM; Abcam) and an increased concentration of NMDA (2.5, 5, and 7.5 μM; Fisher) for episodes of ~30 min at each concentration. The signals were amplified (gain 2000) and bandpass filtered 10 Hz to 5 kHz (Qi-Ying Design). Signals were sampled at 50 kHz (Digidata 1440A, Molecular Devices) and stored on a PC (Axoscope 10.3; Molecular Device) for offline analysis. The amplitude and duration of ENG bursts, the stride duration, the interburst duration, the duty cycle, and the coupling were analyzed on a 300-s epoch (25–60 locomotor cycles) of locomotor-like activity using Spinalcore. The amplitude was measured from the baseline (0) of integrated signals.

Statistics

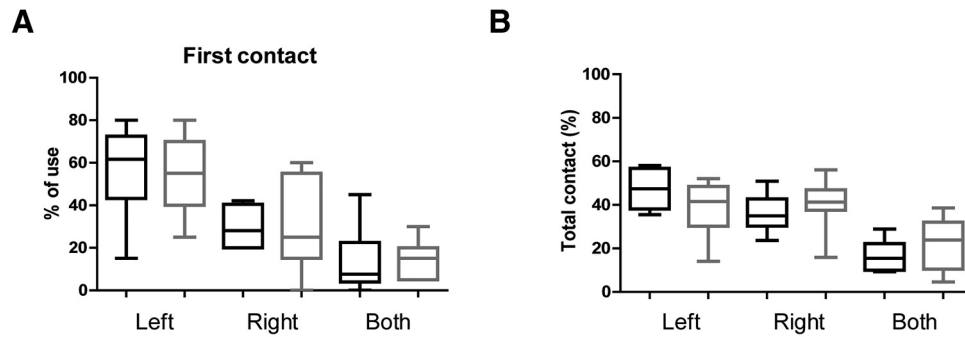
Data for male and female mice were pooled together. Visual inspection suggested that the data were similar between sexes. Circular statistics was used to calculate the robustness of phase couplings between limbs or ENGs during locomotion; Rayleigh values are illustrated as the distance from the center of the polar plot (Drew and Doucet, 1991; Kjaerulff and Kiehn, 1996; Zar, 1996). A phase of 0 (or 1) indicates synchronization, whereas a phase of 0.5 corresponds to an alternation. The statistical significance of phase differences between WT and *Dcc*^{+/-} mice was tested with a Watson–William test. Error bars shown are mean ± SD of the average or the coefficient of variation (CV). The normality of the distribution was assessed with Shapiro–Wilk before two-sample testing. Before pooling data, we tested the homogeneity of variances with a Fisher (two-samples, left and right limb) or Bartlett test (multiple samples, beam and horizontal ladder crossing). To detect differences between the mouse genotypes during adult treadmill locomotion, neonatal locomotor-like activity, and in anatomic measurements, we used the *t* test or nonparametric Mann–Whitney ranked sum test when the variables did not fit a normal distribution (assessed by Kolmogorov–Smirnov test).

Results

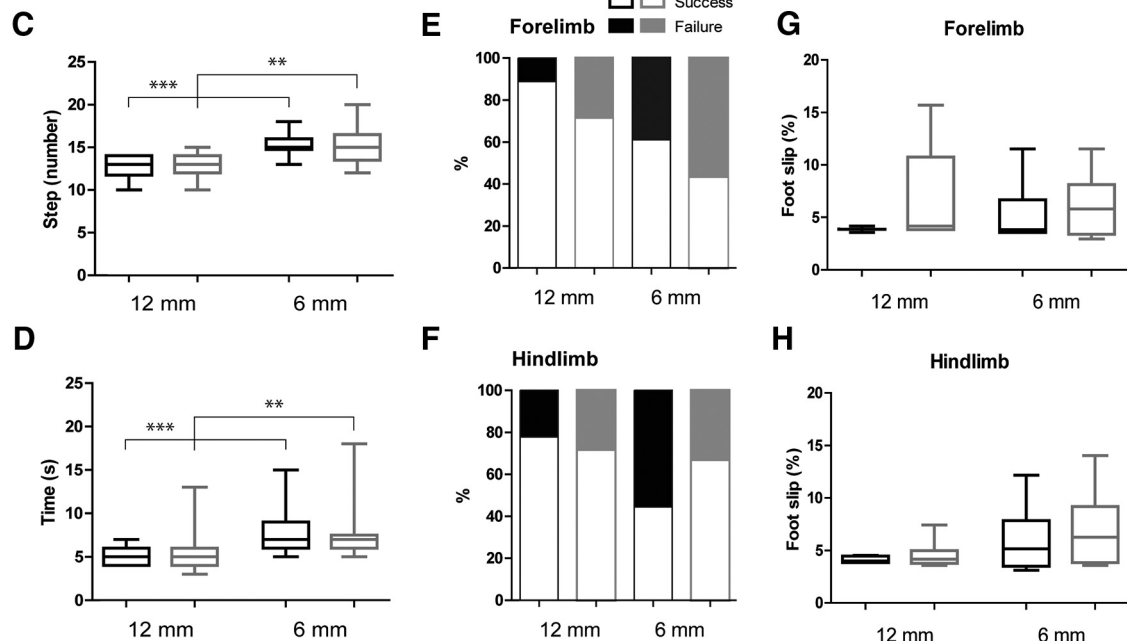
Skilled motor control and locomotion in *Dcc*^{+/-} adult mice

In mice, rats, and cats, while locomotion on a smooth horizontal surface may rely solely on subcortical and spinal motor systems (Z'Graggen et al., 1998; Soblosky et al., 2001), the motor cortex plays an important role in the control of voluntary motor tasks such as skilled forelimb reaching (Whishaw, 2000; Bretzner et al., 2008, 2010; Sparling et al., 2015), as well as skilled locomotion while the animal has to adjust its precise paw and limb trajectory to avoid obstacles (Drew et al., 1996; Metz and Whishaw, 2002; Friel et al., 2007; Laflamme et al., 2019). Previous work showed that *Dcc* protein levels are reduced in the brain of adult *Dcc*^{+/-} mice compared with WT mice (Flores et al., 2005). Using a test of vertical exploration to assess skilled motor control (Fig. 1A,B), we quantified the percentage of initial and subsequent use of left, right, or

Cylinder test



Beam locomotion



Ladder locomotion

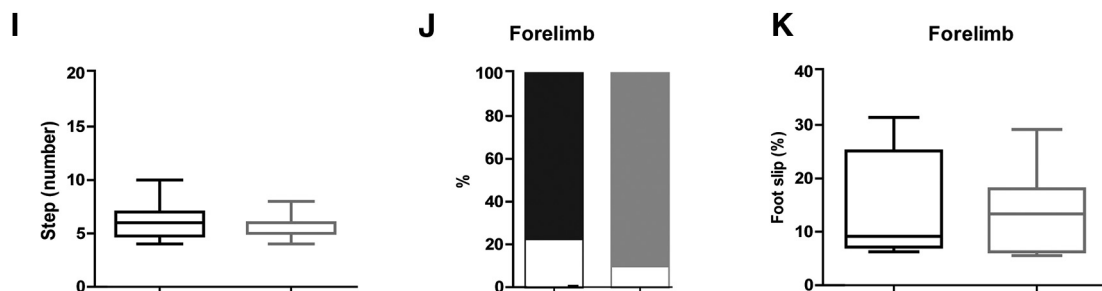


Figure 1. Skilled motor control in adult *Dcc*^{+/-} and WT mice. **A, B**, Percentage of first and total contacts on the wall while rearing in the cylinder test. **C–H**, Mean number of steps (**C**), time (**D**), percentage of successful and failed trials with the forelimb (**E**) and hindlimb (**F**), percentage of foot slips with the forelimb (**G**) and hindlimb (**H**) among trials with errors. **I–K**, Mean number of steps (**I**), percentage of successful and failed trials (**J**), and percentage of foot slips among failed trials (**K**) during locomotion on the rungs of a horizontal ladder. WT in black and *Dcc*^{+/-} in gray; **p* < 0.05, ***p* < 0.01, and ****p* < 0.001 (for statistics, see Extended Data Table 1-1).

both forepaws while reaching the wall of a cylinder during rearing. In comparison to control WT mice, the *Dcc*^{+/-} mice displayed no differences in the percentage of use of their left, right, or both forepaws in the cylinder during the

first contact on the wall (*n* = 6 WT and 7 *Dcc*^{+/-} mice, Mann–Whitney test for left forepaw use, *p* = 0.9226; right forepaw, *p* = 0.6669; and both forepaws, *p* = 0.5163; Fig. 1A), and during the total number of contacts (Mann–

Whitney test for total individual use of the left forepaw, $p=0.2343$; the right forepaw, $p=0.5643$; and both forepaws, $p=0.3534$; Fig. 1B), thus suggesting a normal use of forelimbs during vertical exploration.

To assess balance and motor coordination, we evaluated mice while they walked on a horizontal wide (12-mm width) or narrow (6-mm width) beam (Fig. 1C–H). We first assessed whether there was a learning effect on our measurements on three beam crossings. As there were no significant effects on the number of steps, the time, and the percentage of foot-slips between the three crossings, data were pooled (Fig. 1C,D,G,H, Bartlett or Fischer test, $p > 0.05$; for statistics, see Extended Data Table 1-1). Although both WT and $Dcc^{+/-}$ mice took more steps to cross the narrow beam than the wide one ($n = 6 \times 3$ WT and 7×3 $Dcc^{+/-}$ crossings, Mann–Whitney test, $p=0.0001$ for WT and $p=0.0011$ for $Dcc^{+/-}$ on the 6- vs 12-mm beam; Fig. 1C), no statistical differences were observed according to genotype (Mann–Whitney test, $p=0.8392$ for WT vs $Dcc^{+/-}$ on the 6-mm beam; and $p=0.3193$ for WT vs $Dcc^{+/-}$ on the 12-mm beam; Fig. 1C). Similarly, the time to cross the wide beam was significantly shorter than to cross the narrow beam (Mann–Whitney test, $p=0.0002$ for WT and $p=0.0011$ for $Dcc^{+/-}$ on the 6- vs 12-mm beam; Fig. 1D); nevertheless, no differences were found according to genotype (Mann–Whitney test, $p=0.6145$ for WT vs $Dcc^{+/-}$ on the 6-mm beam; $p=0.8249$ for WT vs $Dcc^{+/-}$ on the 12-mm beam; Fig. 1D). The proportion of successful/failed crossings was not significantly different while crossing the wide or the narrow beam with the forelimbs (Mann–Whitney test, $p=0.1398$ for the WT forelimbs and $p=0.1626$ for the $Dcc^{+/-}$ forelimbs on the 6- vs 12-mm beam; Fig. 1E) or the hindlimbs (Mann–Whitney test $p=0.1534$ for the WT hindlimbs and $p=0.9456$ for the $Dcc^{+/-}$ hindlimbs on the 6- vs 12-mm beam; Fig. 1F). Among the failed crossings, the percentage of foot-slips was not significantly different with the forelimbs on the narrow beam ($n=7/18$ WT and $12/21$ $Dcc^{+/-}$ crossings, Mann–Whitney test, $p=0.8322$; Fig. 1G) or the hindlimbs on the narrow or wide beam ($n=10/18$ WT and $7/21$ $Dcc^{+/-}$ crossings on the narrow beam, Mann–Whitney test, $p=0.4336$; $n=4/18$ WT and $6/21$ $Dcc^{+/-}$ crossings on the wide beam, Mann–Whitney test, $p=1$; Fig. 1H) according to mouse genotype, thus supporting a proper locomotor balance and motor coordination in $Dcc^{+/-}$ mice.

To evaluate whether skilled forelimb locomotion might be impaired on Dcc mutation, we also assessed mice while crossing a horizontal ladder with even-spaced rungs, a situation where there is a need for precise limb trajectories and paw placements. (Fig. 1I–K). As with beam locomotion, we assessed whether there was a learning effect over the subsequent crossings. As there was no significant effect on the number of steps and the percentage of foot-slips over three crossings (Fig. 1I,J, Bartlett test, $p > 0.05$; for statistics, see Extended Data Table 1-1), data were pooled. Both WT and $Dcc^{+/-}$ mice exhibited no statistical differences in the number of steps and in the percentage of foot-slips while walking on the rungs of the horizontal ladder (Mann–Whitney test for the

number of steps of $n=18$ WT vs 21 $Dcc^{+/-}$ crossings, $p=0.8840$; Mann–Whitney test for the proportion of successful vs failed crossings, $p=0.6614$; Fig. 1I). Among failed crossings, the percentage of foot-slips with the forelimb was also not significantly different according to genotype (Mann–Whitney test, $p=0.4091$; Fig. 1K). Taken together, $Dcc^{+/-}$ mice display normal posture and balance overall, as well as normal skilled forelimb coordination and placement during skilled locomotion on a beam or a ladder.

Anatomy of the corticospinal tract in the adult mouse

A single-allele Dcc mutation is sufficient to alter pyramidal decussation and induce an aberrant bilateral misprojection of the corticospinal tract in humans (Srouf et al., 2010; Welniarz et al., 2017). Thus, we asked whether a heterozygous Dcc mutation in mice might also be sufficient to impair normal projection of the corticospinal tract. As shown in Figure 2, axonal tract tracing of the motor cortex revealed that the projection of corticospinal axons at the level of the pyramidal decussation (Fig. 2B, middle panels) or postdecussation were similar in both $Dcc^{+/-}$ and WT mice (Fig. 2B, right-most panels, five adult WT and five $Dcc^{+/-}$ animals), suggesting that the corticospinal tract projects normally in adult $Dcc^{+/-}$ mice. These results are consistent with previous observations (Welniarz et al., 2017).

Functional connectivity of the corticospinal tract in the adult mouse

While our anatomic studies revealed that corticospinal tract projection appears normal in $Dcc^{+/-}$ mice, the cortical representation and/or functional connectivity could still be impaired and evoke aberrant bilateral or ipsilateral movements in both forelimb and hindlimb muscles. To test this hypothesis, we recorded motor and EMG responses from bilateral forelimb and hindlimb muscles evoked by ICMS in the cortical caudal forelimb and hindlimb areas of adult WT and $Dcc^{+/-}$ adult mice. As shown in Figure 3A, ICMS applied within the cortical representation of the hindlimb evoked the strongest EMG responses in the contralateral hindlimb muscle, TA, and weaker responses in the ipsilateral TA muscle of WT and $Dcc^{+/-}$ mice at supra-threshold. To assess changes in corticospinal efficacy, we compared the threshold of cortically evoked motor responses in contralateral $Dcc^{+/-}$ and WT forelimb BB and hindlimb TA muscles. Overall, there was no difference in the thresholds for evoking EMG responses in contralateral WT and $Dcc^{+/-}$ forelimb and hindlimb muscles (Mann–Whitney test: $n=7$ WT and 6 $Dcc^{+/-}$ for the TA, $p=0.50$; and $n=5$ WT and 5 $Dcc^{+/-}$ for the BB, $p=0.34$; Fig. 3B). Moreover, the threshold for evoking contralateral motor responses in both forelimb and hindlimb was lower than that for evoking ipsilateral motor responses (Wilcoxon signed rank test: $n=4$ WT-Forelimbs, $p=0.12$; 2 $Dcc^{+/-}$ -Forelimbs, $p=0.5$; 11 WT-Hindlimbs, $p=9.7 \times 10^{-4}$; 13 $Dcc^{+/-}$ -Hindlimbs $p=4.9 \times 10^{-4}$; Fig. 3C), consistent with a proper contralateral projection of the corticospinal tract. In pairs of muscles

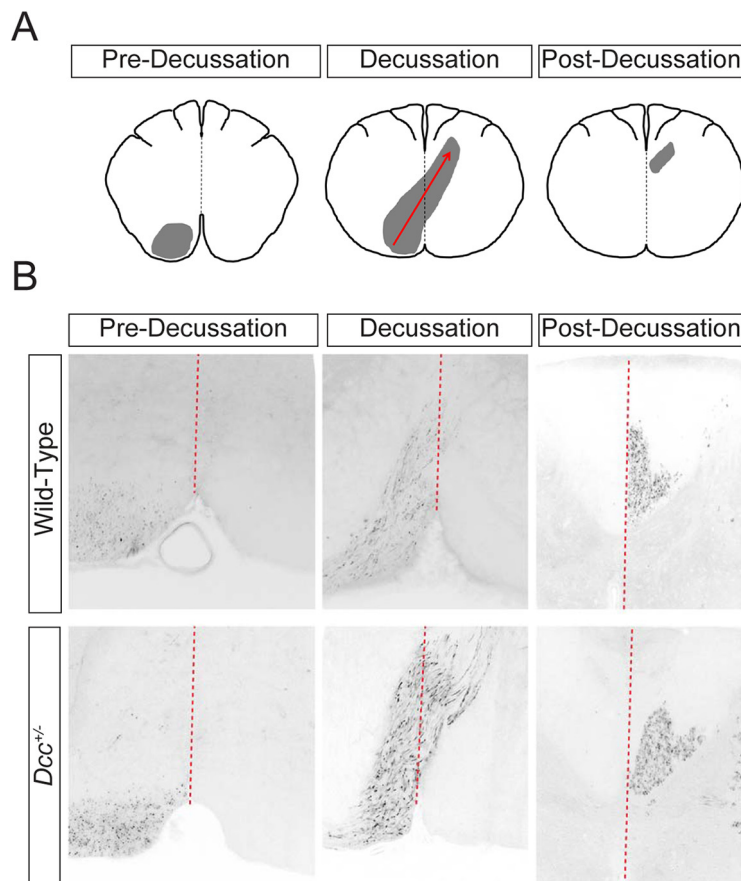


Figure 2. Projections of the corticospinal tract in $Dcc^{+/-}$ and WT mice. **A**, Schematic drawing of transverse brainstem sections showing a unilateral corticospinal tract axon bundle (gray area) as it projects from the left motor cortex to the contralateral dorsal funiculus. **B**, BDA tracing of the corticospinal tract of three-month-old WT and $Dcc^{+/-}$ mice shows no difference in the projection of corticospinal tract axons at the level of the pyramidal decussation.

recorded with EMGs, we found that the ipsilateral side was less excitable, sometimes not even reaching the threshold criterion in contrast to the contralateral side in both WT and $Dcc^{+/-}$ mice ($n=6$ WT and 6 $Dcc^{+/-}$ mice; Fig. 3D). When there were sufficient ipsilateral EMG responses around the threshold, we calculated latencies on both the ipsilateral and contralateral side (Mann–Whitney test, $n=4$ pairs, $p=0.74$; Fig. 3E). Latencies of ipsilateral EMG responses occurred systematically after contralateral ones, but no differences were found between WT and $Dcc^{+/-}$ mice. The strength of the response was evaluated as the number of motor spikes evoked on ICMS. Although the number of motor spikes in contralateral muscles appeared higher than in ipsilateral ones, it was not statistically different according to genotype (Wilcoxon signed rank test for contralateral vs ipsilateral responses: $n=6$ WT, $p=0.22$ and $n=6$ $Dcc^{+/-}$, $p=0.31$. Mann–Whitney test for WT vs $Dcc^{+/-}$: contralateral side, $p=0.31$; ipsilateral side, $p=1$; Fig. 3F). Furthermore, ICMS applied within the cortical representation of the hindlimb evoked specific motor responses in hindlimb muscles, but never in forelimb muscles, in the mutant mice (data not shown) and conversely the cortical representation of the forelimb never evoked any responses in hindlimb muscles, thus demonstrating that corticospinal projections maintain

their specificity. Together, these results show that the projection and functional connectivity of the corticospinal tract are preserved in adult $Dcc^{+/-}$ mice.

Treadmill locomotion in the adult mouse

Although $Dcc^{+/-}$ mice do not show impaired gross voluntary motor and locomotor behaviors, we hypothesized that the loss of one Dcc allele might cause more subtle changes in locomotor pattern and rhythm. To test that, we performed gait analysis of WT and $Dcc^{+/-}$ mice during treadmill locomotion at steady speeds of 15, 20, and 30 cm/s. Overall, the mean and CV of the step cycle duration, the swing duration, the stance duration, and the duty cycle of the stance phase decreased as a function of treadmill speed for both WT and $Dcc^{+/-}$ mice (Fig. 4). Although the duration of the step cycle and stance phase was normal, the duty cycle of the stance phase was significantly increased in $Dcc^{+/-}$ mice in comparison to their WT littermates at low and intermediate treadmill speeds (Fig. 4D, $n=8$ WT and 10 $Dcc^{+/-}$ mice, duty cycle, Mann–Whitney test, $p=0.0085$ at 15 cm/s; unpaired Student's t test, $p=0.0490$ at 20 cm/s; for statistics, see Extended Data Table 4-1). Moreover, we also found a significant decrease in the variability of the duty cycle of the stance

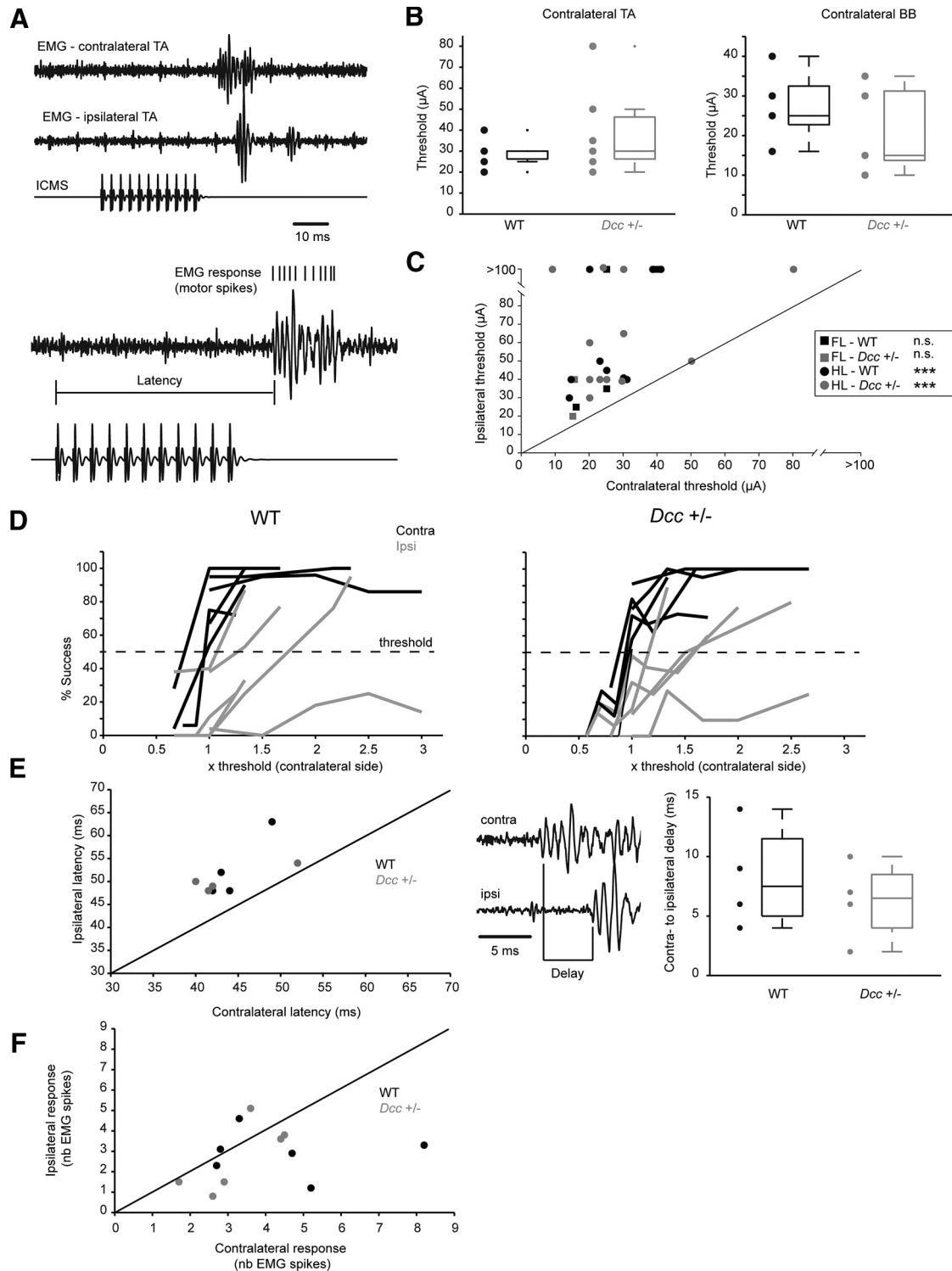


Figure 3. $Dcc^{+/-}$ adult mice exhibit normal lateralization of the corticospinal tract. **A**, Examples of EMG activity of contralateral and ipsilateral TA. A 30-ms train of cathodal pulses (duration 0.2 ms, interval 2.8 ms) was delivered in either the caudal forelimb area or the hindlimb area. Bottom, Higher temporal resolution of the contralateral trace illustrates latency and response (motor spikes raster) measurements. **B**, left, Threshold for evoking activity in the contralateral BB (BB). Right, Threshold for evoking activity in the contralateral TA. Threshold is defined as motor spikes elicited in at least 50% of the trials. **C**, Thresholds for pairs of hindlimbs (HL; circle) or forelimbs (FL; square). Contralateral is on the x-axis and ipsilateral on the y-axis. **D**, Success rate (percentage) for evoking an EMG response versus the threshold of the contralateral side. Dashed line indicates the threshold, defined as a success rate of 50%. Data are for pairs of muscle recorded with EMGs. Contralateral is in black and ipsilateral in gray. **E**, left, Ipsilateral versus contralateral averaged latencies for pairs of muscles recorded with EMGs. Middle, An example of EMG traces to illustrate the delay between

continued

contralateral and ipsilateral sides. Right, Boxplot of contralateral to ipsilateral delays. **F**, Averaged number of motor spikes evoked by ICMS for the contralateral (x-axis) and ipsilateral (y-axis) sides. WT in black and *Dcc*^{+/-} in gray; *** *P* < 0.001.

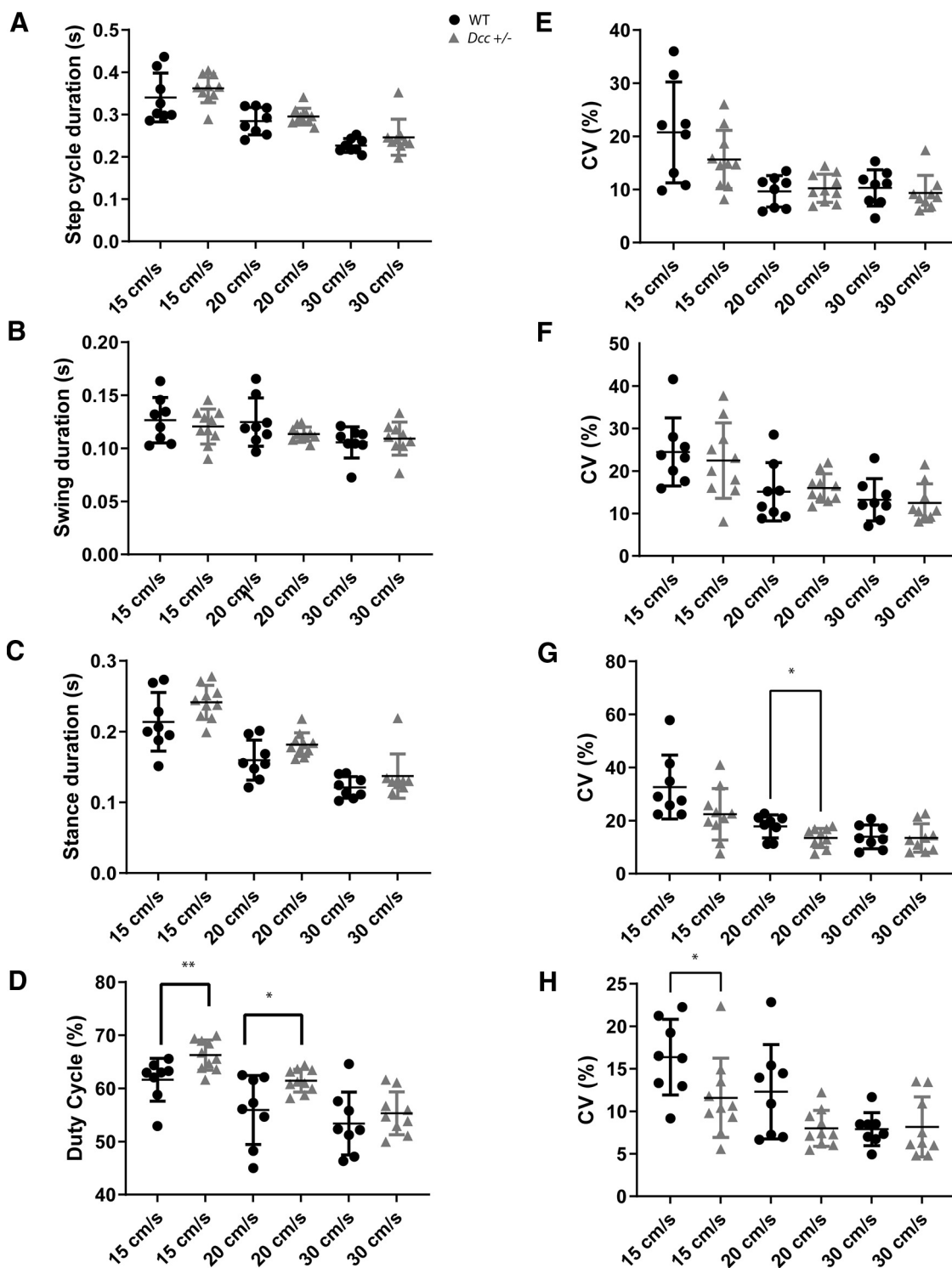


Figure 4. Locomotor pattern of adult *Dcc*^{+/-} and WT mice during treadmill locomotion. **A–D**, Mean and **(E–H)** CV of step cycle duration **(A, E)**, swing duration **(B, F)**, stance duration **(C, G)**, and duty cycle of the stance phase **(D, H)** of WT and *Dcc*^{+/-} mice at three different treadmill speeds (15, 20, and 30 cm/s). WT in black and *Dcc*^{+/-} in gray; **p* < 0.05 and ***p* < 0.01 (for statistics, see Extended Data Table 4-1).

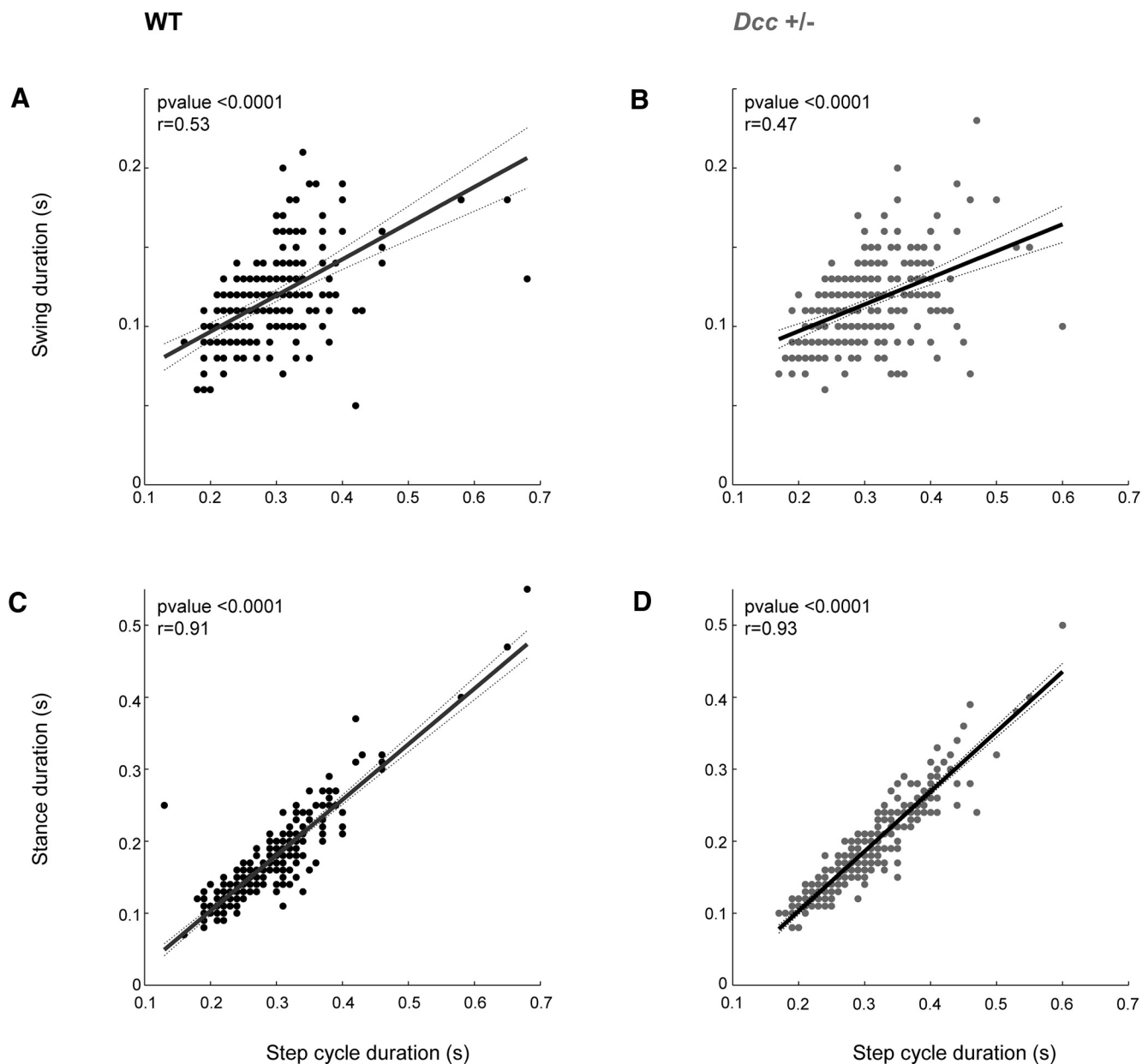


Figure 5. Swing and stance duration as functions of step cycle duration during treadmill locomotion. Swing (top panels, **A**, **B**) and stance (bottom panels, **C**, **D**) duration as functions of step cycle duration of WT and *Dcc*^{+/-} mice. Note three different treadmill speeds were combined. WT in black and *Dcc*^{+/-} in gray.

phase in *Dcc*^{+/-} mice in comparison to WT at 15 cm/s (Fig. 4H, $n=8$ WT and 10 *Dcc*^{+/-} mice, duty cycle, unpaired t test, $p=0.0420$ at 15 cm/s; for statistics, see Extended Data Table 4-1). To look for changes in locomotor pattern as function of speed, we then plotted the duration of the stance and swing phase as function of step cycle duration. The linear regression did not show any significant differences according to genotype ($n=8$ WT and 10 *Dcc*^{+/-} mice, F test on slopes, $p=0.0503$, $F_{(1,497)}=3.85$; Fig. 5), thus suggesting overall a normal locomotor pattern in the *Dcc* heterozygous mice.

Given the bilateral locomotor disorganization in *Dcc* homozygous mutant spinal cords (Rabe Bernhardt et al., 2012), we also investigated the bilateral and homolateral

coupling of limbs during treadmill locomotion. As shown by their polar plots (Fig. 6A–C), the coupling between left-right forelimbs and hindlimbs, as well as the homolateral coupling between forelimbs and hindlimbs, were normal in *Dcc*^{+/-} mice in comparison to their WT littermates (Watson–William test of WT vs *Dcc*^{+/-}: hindlimb coupling, $p=0.71$ at 15 cm/s, $p=0.70$ at 20 cm/s and $p=0.99$ at 30 cm/s; WT vs *Dcc*^{+/-}: forelimb coupling, $p=0.77$ at 15 cm/s, $p=0.99$ at 20 cm/s and $p=0.71$ at 30 cm/s; WT vs *Dcc*^{+/-}: homolateral coupling, $p=0.98$ at 15 cm/s, $p=0.69$ at 20 cm/s and $p=0.95$ at 30 cm/s). We also looked at phase coupling as function of locomotor frequency, which shows that the coordination between left and right forelimbs and hindlimbs was normal overall in

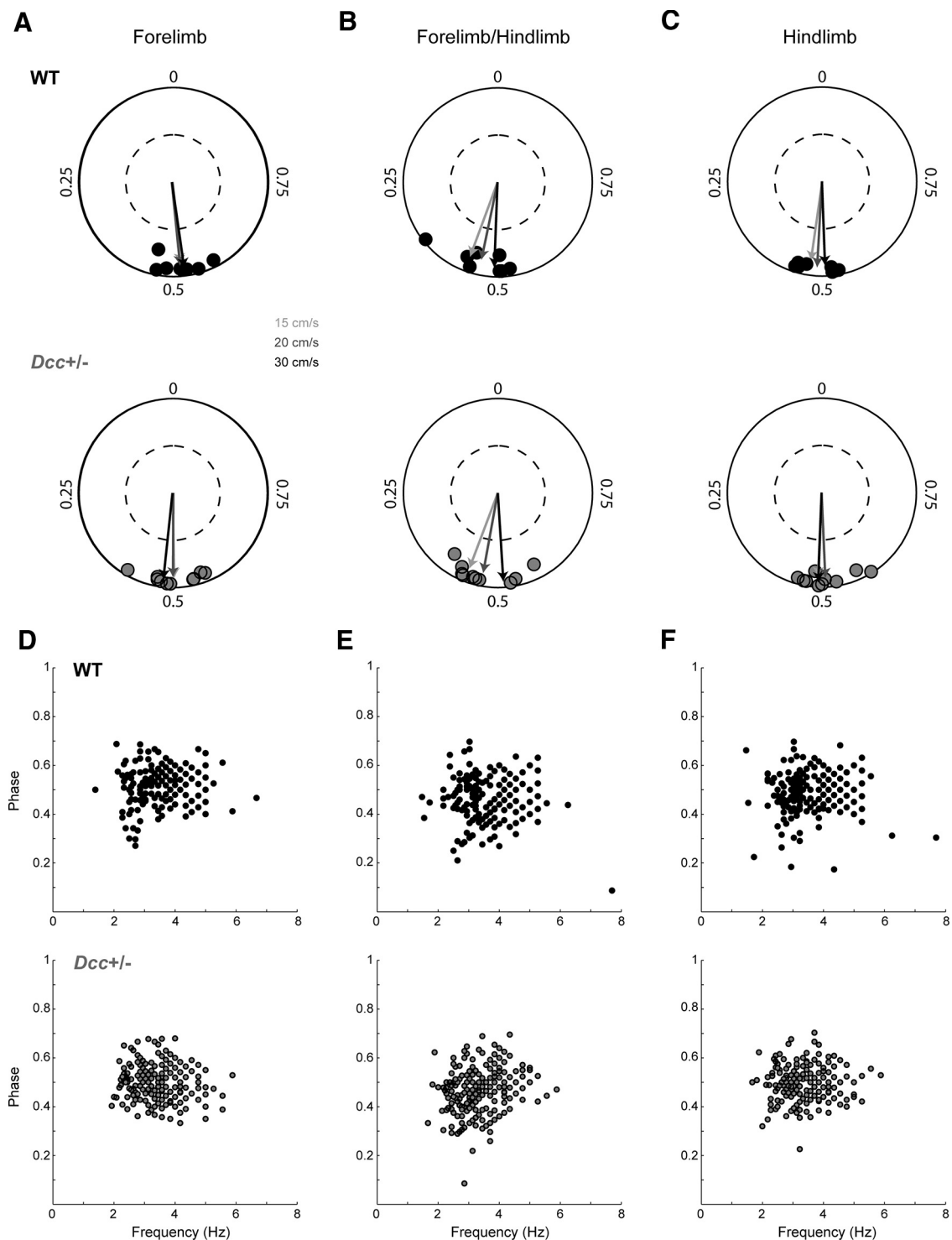


Figure 6. Bilateral and homolateral interlimb coordination during treadmill locomotion. **A–C**, Polar plots showing the mean vector for the relationships between left and right forelimbs (**A**), left and right hindlimbs (**C**), and between homolateral forelimb and hindlimb (**B**) of WT (black circles) and *Dcc*^{+/-} (gray circles) at treadmill speeds of 15, 20, and 30 cm/s. The position on the polar plot indicates mean phase; the distance from the center of the polar plot indicates strength of the coupling (Rayleigh). Symbols represent individual mice at a treadmill speed of 20 cm/s, vectors represent the mean phase coupling of WT and *Dcc*^{+/-} groups at 15, 20, and 30 cm/s. Dashed inner circles represent a Rayleigh value of 0.5. **D–F**, Phase of the coupling between left and right forelimbs (**D**), hindlimbs (**F**), and (**E**) forelimb-hindlimb as a function of locomotor frequency during treadmill locomotion at 15–30 cm/s. WT in black and *Dcc*^{+/-} in gray.

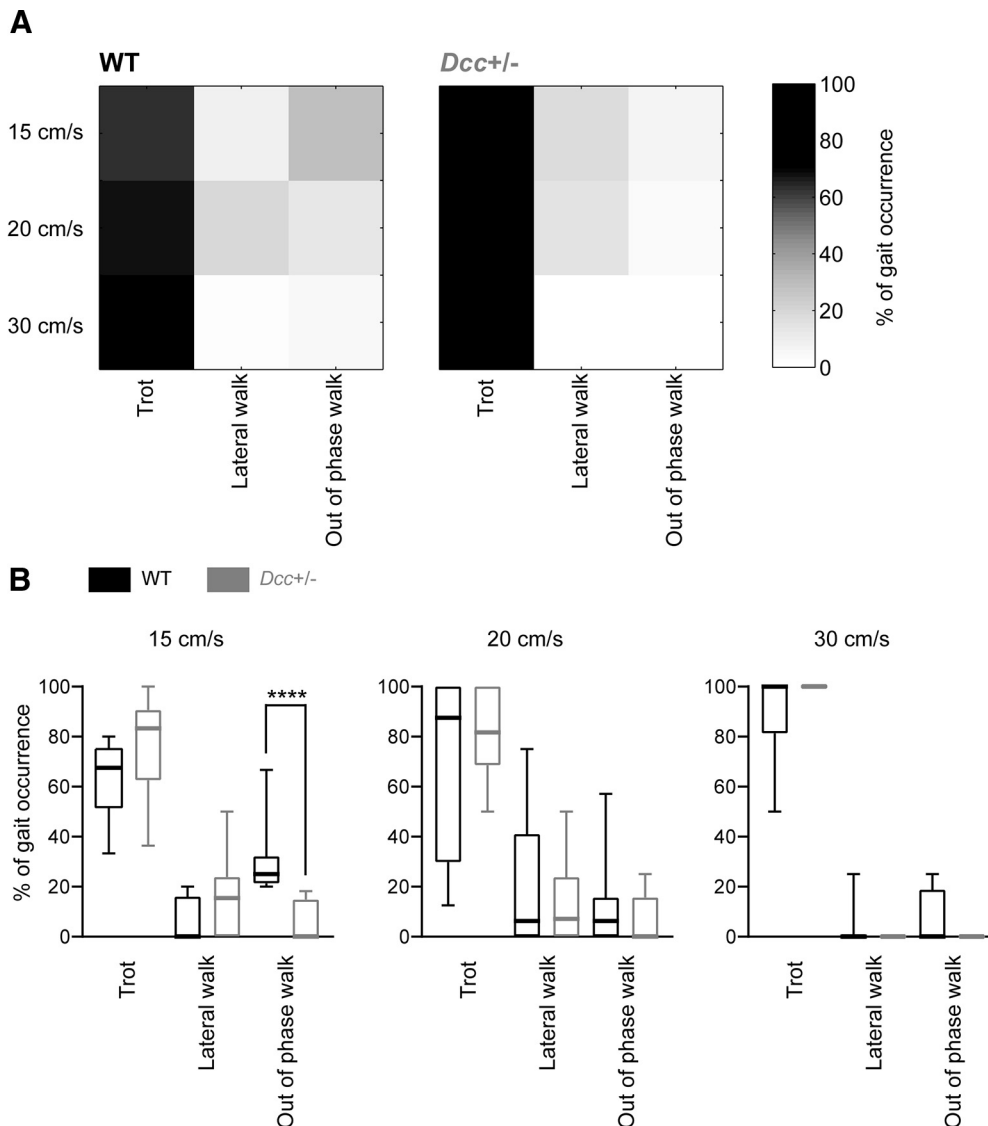


Figure 7. Locomotor gait occurrence during treadmill locomotion. **A**, Gray-scaled matrixes of the percentage of occurrence of a gait (column) at 15, 20, and 30 cm/s (row) for WT and *Dcc*^{+/-} mice. The sum of a row equals 100%. **B**, Box plots representing the percentage of gait occurrence at 15, 20, and 30 cm/s; **** $p < 0.0001$.

Dcc^{+/-} mice during locomotion at treadmill speeds from 15 to 30 cm/s (Fig. 6D–F). Overall, these results show that locomotor pattern, rhythm, and interlimb coordination of *Dcc*^{+/-} adult mice are normal.

As their WT littermates, *Dcc*^{+/-} mice exhibited out-of-phase walk (i.e., asymmetrical walk), lateral walk, and trot with the predominance of trot at the highest treadmill speed tested of 30 cm/s (Fig. 7). Interestingly, *Dcc*^{+/-} mice exhibited significantly less out-of-phase walk than their WT littermates at the slowest treadmill speed of 15 cm/s ($n = 8$ WT and 10 *Dcc*^{+/-}, Mann–Whitney test, $p < 0.0001$ at 15 cm/s; Fig. 7B); nevertheless, its occurrence normalized at higher treadmill speeds of 20 and 30 cm/s (no significant differences between *Dcc*^{+/-} and WT mice; Fig. 7B). Taken together, these analyses suggest that the repertoire of gaits was overall normal in *Dcc*^{+/-} mice.

Locomotor pattern and rhythm during neonatal locomotor-like activity

Given that motor and locomotor controls appear to be normal in adult *Dcc*^{+/-} mice, we then assessed whether the loss of one WT allele of *Dcc* could impair the function of isolated local spinal locomotor circuits. We first verified whether *Dcc*^{+/-} developing spinal cords have reduced *Dcc* protein levels. Western blotting showed that *Dcc* protein levels are reduced by ~50% in *Dcc*^{+/-} embryonic spinal cords compared with WT spinal cords ($n = 6$ embryos per genotype, Mann–Whitney test, $p = 0.002$; Fig. 8). This is consistent with what has been observed previously in adult *Dcc*^{+/-} mouse spinal cords (Liang et al., 2014).

We next assessed whether the loss of one WT allele of *Dcc* could impair the function of isolated local spinal locomotor circuits. To test this, we used spinal cords isolated

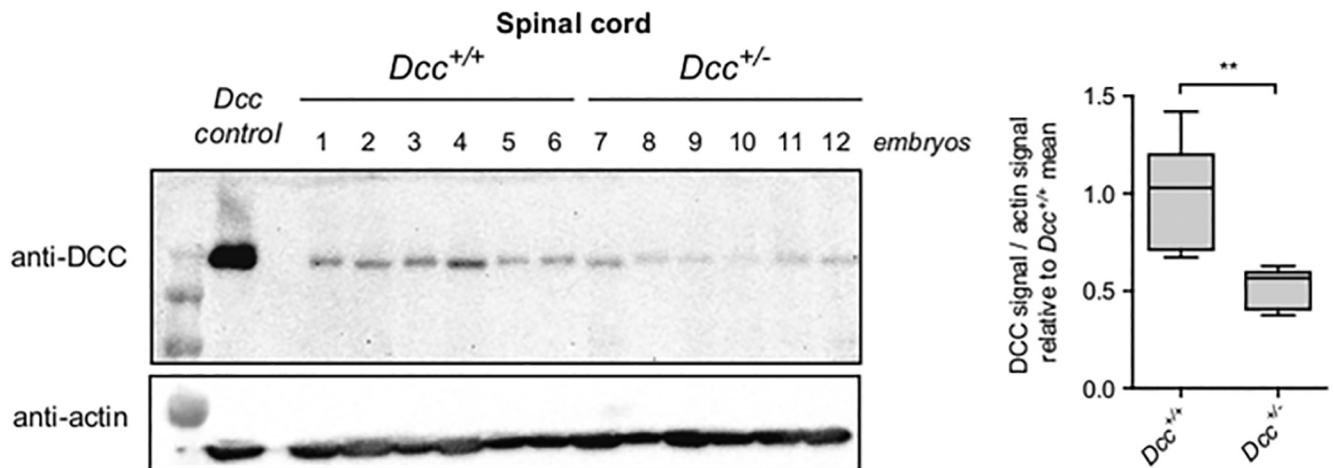


Figure 8. Dcc protein levels in $Dcc^{+/-}$ and WT spinal cords. Left, Western blotting of Dcc in embryonic WT and $Dcc^{+/-}$ spinal cords. *Dcc control* is a cell lysate overexpressing a *Dcc* cDNA. Right, Dcc/actin ratio relative to WT ($Dcc^{+/-}$); ** $p < 0.01$.

from neonatal WT and $Dcc^{+/-}$ mice, thus allowing us to study spinal circuits without the influence of descending or peripheral input. As previously described (Kudo and Yamada, 1987; Cazalets et al., 1992), locomotion was triggered by bath application of a cocktail of $8 \mu\text{M}$ 5HT and $2.5, 5,$ or $7.5 \mu\text{M}$ NMDA to challenge spinal interneuronal excitability. As illustrated by ENG bursts of L2 and L5 lumbar ventral root activities (Fig. 9A,B), locomotor-like activity was evoked at a low concentration of $2.5 \mu\text{M}$ NMDA, but the activity was more regular and stable at an intermediate concentration of $5 \mu\text{M}$ before decreasing in amplitude at a high concentration of $7.5 \mu\text{M}$ in both WT and $Dcc^{+/-}$ mutant spinal cords (Fig. 9F). Increasing the concentration of NMDA statistically decreased the cycle duration, which translated into an increased duty cycle in both L2 and L5 ENG bursts for both WT and $Dcc^{+/-}$ spinal cords (Fig. 9D). Nevertheless, no significant changes were found in cycle duration, burst duration, or duty cycle regarding the mouse genotype (for statistics, see Extended Data Table 9-1), thus suggesting normal functioning of the spinal interneuronal circuit in $Dcc^{+/-}$ mice.

As shown in both WT and $Dcc^{+/-}$ spinal cord examples (Fig. 9A,B), the ENG burst amplitude in L2 and L5 increased as a function of NMDA concentration from 2.5 to $5 \mu\text{M}$ and tended to decrease at a high concentration of $7.5 \mu\text{M}$, below the amplitude level evoked at $2.5 \mu\text{M}$. Interestingly, the amplitude of the L2 ENG burst of $Dcc^{+/-}$ spinal cords was significantly higher than that of WT regardless of NMDA concentration (Fig. 9F, $n = 4$ WT and 7 $Dcc^{+/-}$, burst amplitude of WT vs $Dcc^{+/-}$ L2 ENGs, Mann–Whitney test, $p = 0.0424$ at $2.5 \mu\text{M}$, $p = 0.0424$ at $5 \mu\text{M}$, $p = 0.0242$ at $7.5 \mu\text{M}$; for statistics, see Extended Data Table 9-1). This increased motor output suggests that the spinal locomotor circuit (at least in the L2 segment) is more excitable on bath application of NMDA in the developing spinal cord on loss of one *Dcc* allele.

Variability in locomotor pattern and rhythm during neonatal locomotor-like activity

As previously shown in some mutant mouse studies (Zhang et al., 2008), $Dcc^{+/-}$ mutation might translate into

a higher variability in locomotor pattern and rhythm during locomotion. To test this hypothesis, we quantified the CV in locomotor features (Fig. 10). Although ENG waveforms were more variable at low concentrations of NMDA (Fig. 9A,B), overall, there were no significant differences in the variability of cycle duration, burst duration, burst amplitude, and duty cycle (Fig. 10A, $n = 4$ WT and 7 $Dcc^{+/-}$, Mann–Whitney test for L2 cycle duration, $p = 0.0242$; for statistics, see Extended Data Table 10-1). Only the cycle duration of the L2 ENG waveform showed significantly higher variability in the $Dcc^{+/-}$ cycle duration of the L2 ENG in comparison to the WT.

Left-right and flexor-extensor coordination during neonatal locomotor-like activity

Although some mutant mice can produce a more variable locomotor coordination (Zhang et al., 2008), others produce a less variable one (Bellardita and Kiehn, 2015). As illustrated by polar plots (Fig. 11; for statistics, see Extended Data Table 11-1), the coordination between left-right flexor (Fig. 11A), left-right extensor (Fig. 11B), and flexor-extensor (Fig. 11C) related ventral root activities were not significantly different according to the genotype (Watson–William test of WT vs $Dcc^{+/-}$: left-right L2 coupling, $p = 0.742$ at $2.5 \mu\text{M}$, $p = 0.890$ at $5 \mu\text{M}$ and $p = 0.973$ at $7.5 \mu\text{M}$; WT vs $Dcc^{+/-}$: left-right L5 coupling, $p = 0.880$ at $2.5 \mu\text{M}$, $p = 0.954$ at $5 \mu\text{M}$ and $p = 0.582$ at $7.5 \mu\text{M}$; WT vs $Dcc^{+/-}$: right L2-L5 coupling, $p = 0.705$ at $2.5 \mu\text{M}$, $p = 0.840$ at $5 \mu\text{M}$ and $p = 0.894$ at $7.5 \mu\text{M}$). The variability of the coupling was not affected in $Dcc^{+/-}$ mice as evaluated with Mann–Whitney tests on Rayleigh values of WT versus $Dcc^{+/-}$ left-right L2 coupling: $p = 0.527$ at $2.5 \mu\text{M}$, $p = 0.527$ at $5 \mu\text{M}$, and 0.109 at $7.5 \mu\text{M}$ (Fig. 11D); WT versus $Dcc^{+/-}$ left-right L5 coupling: $p = 0.629$ at $2.5 \mu\text{M}$, $p = 0.629$ at $5 \mu\text{M}$, and 0.857 at $7.5 \mu\text{M}$ (Fig. 11E); WT versus $Dcc^{+/-}$ rL2-rL5 coupling, $p = 0.230$ at $2.5 \mu\text{M}$, $p = 0.412$ at $5 \mu\text{M}$, and 0.648 at $7.5 \mu\text{M}$ (Fig. 11F). Overall, these results suggest a normal flexor-extensor and left-right coordination regardless of the NMDA concentrations in $Dcc^{+/-}$ spinal cord preparations.

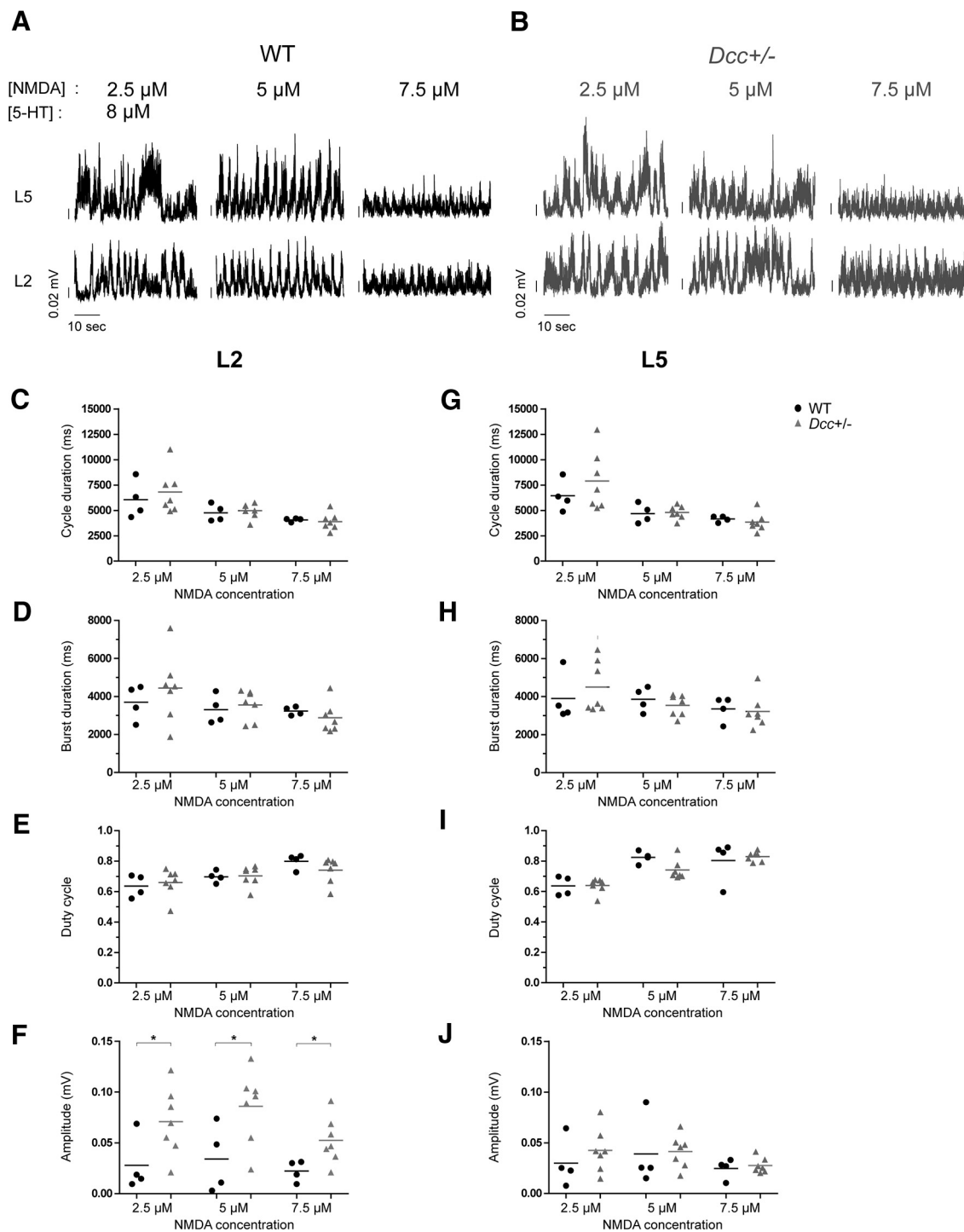


Figure 9. Locomotor pattern and rhythm during neonatal locomotor-like activity. **A, B**, Examples of L5 and L2 ENG recordings of WT (**A**) and *Dcc*^{+/-} (**B**) mice on bath application of drugs (8 μ M 5HT and 2.5, 5, or 7.5 μ M NMDA). **C–J**, Mean and data of cycle duration (**C, G**), burst duration (**D, H**), duty cycle (**E, I**), and burst amplitude (**F, J**) of WT and *Dcc*^{+/-} L2 (**C–F**) and L5 (**G–J**) ENG at different NMDA concentrations (8 μ M 5HT and 2.5, 5, or 7.5 μ M NMDA); **p* < 0.05 (for statistics, see Extended Data Table 9-1).

Discussion

We show that adult mice lacking one allele of functional *Dcc* do not show impairments in skilled motor and locomotor control. In contrast to human individuals who have heterozygous *DCC* mutations, *Dcc* heterozygosity in mice does not promote an aberrant bilateral projection of the

corticospinal tract or prevents its normal contralateral projection. The integrity of cortical representations and the functional connectivity of the corticospinal tract to forelimb and hindlimb motoneuronal pools are also preserved in *Dcc*^{+/-} mice. On the other hand, although treadmill locomotion is mostly normal, the loss of one *Dcc*

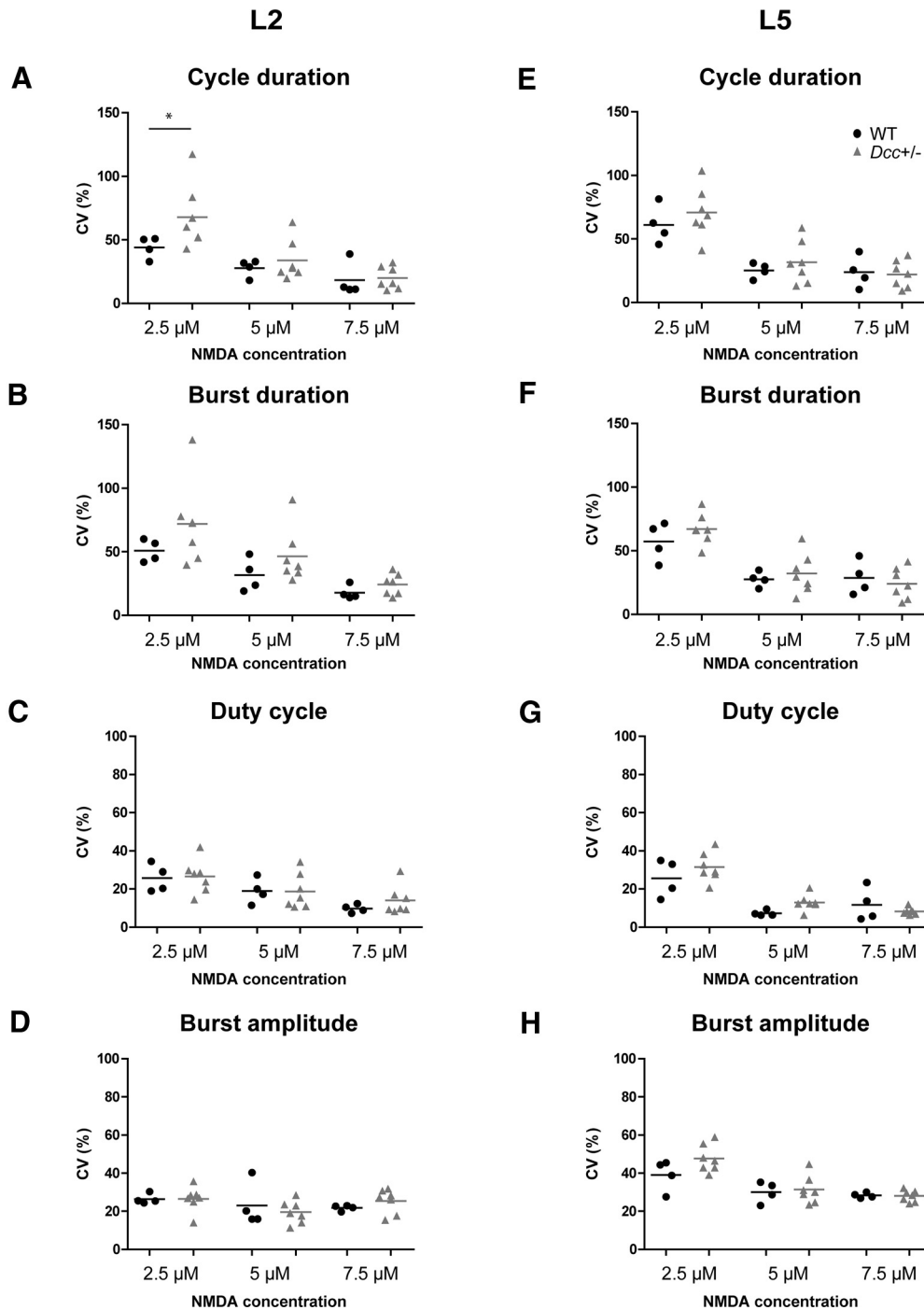


Figure 10. Variability in ENG waveforms during neonatal locomotor-like activity. Mean and CVs of cycle duration (**A, E**), burst duration (**B, F**), duty cycle (**C, G**), and burst amplitude (**D, H**) of WT (black circles) and *Dcc*^{+/-} (gray triangles) of L2 (**A-D**) and L5 (**E-H**) ENG waveforms at different NMDA concentrations; **p* < 0.05 (for statistics, see Extended Data Table 10-1).

allele increases the duration and duty cycle of the stance phase, suggesting sensory feedback impairment. Moreover, although the spinal locomotor circuit appears functionally normal, *Dcc* heterozygous mutation increases the output of the flexor-related motoneuronal pool of isolated neonatal spinal cords. In summary, the heterozygous *Dcc* mouse does not replicate the motor phenotype of people affected with *DCC*

haploinsufficiency, but it exhibits subtle motor differences that have not been reported so far.

Skilled motor control, motor cortex, and its corticospinal tract in adult *Dcc*^{+/-} mice

Although the corticospinal tract and connectivity in the mouse are different from that of the human, previous

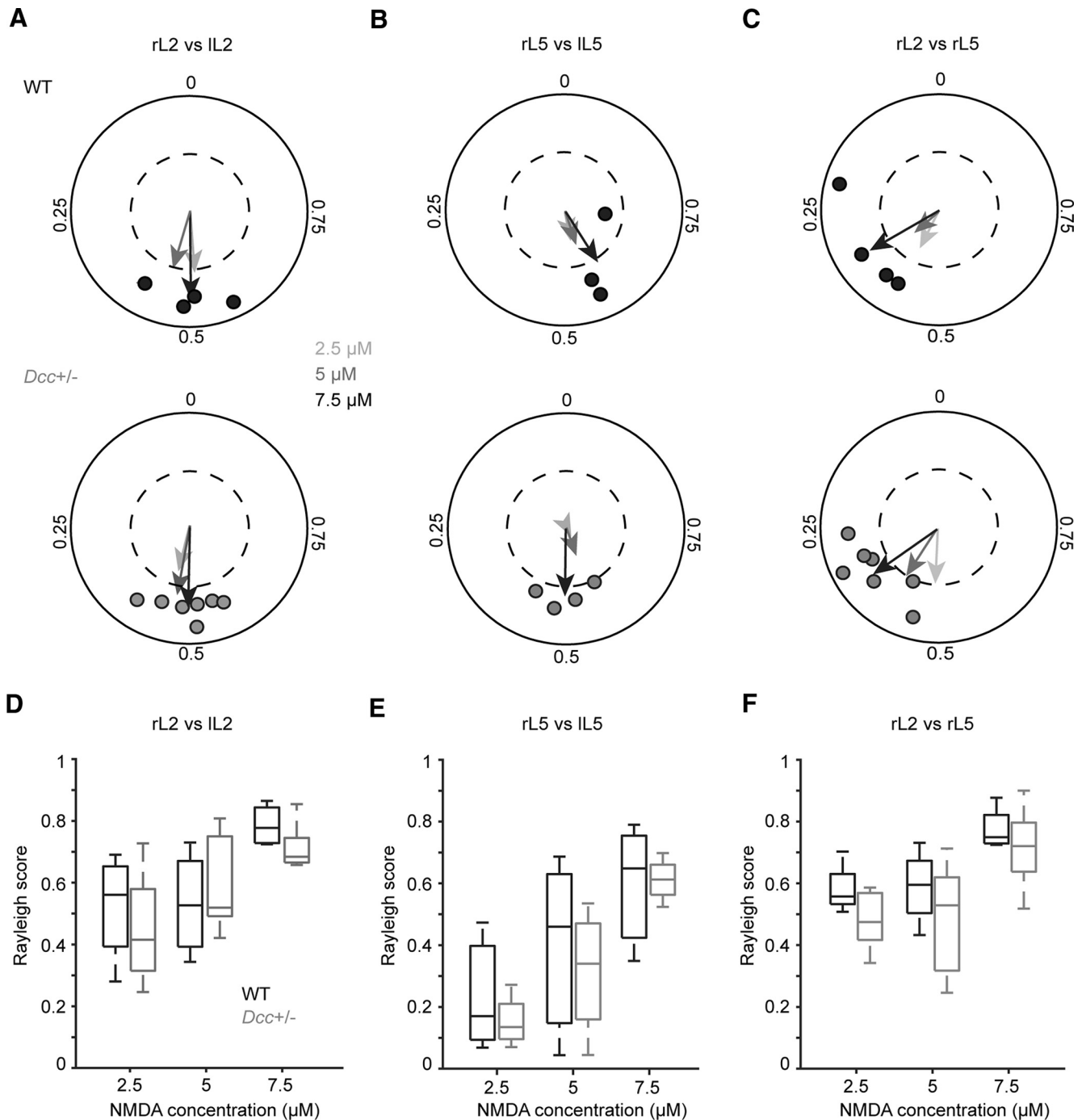


Figure 11. Locomotor coupling during neonatal locomotor-like activity. **A–C**, Polar plots showing the mean vector (arrows) for the relationships between left and right L2 (**A**, IL2 vs rL2) and L5 (**B**, IL5 vs rL5), and between homolateral flexor and extensor (**C**, rL2 vs rL5) of WT (top polar plots) and *Dcc*^{+/-} (bottom polar plots) spinal cord preparations at low (2.5 μM, lighter gray arrow), intermediate (5 μM, darker gray arrow), and high (7.5 μM, black arrow) NMDA concentrations. The position on the polar plot indicates mean phase; the distance from the center of the polar plot indicates strength of the coupling (Rayleigh). For clarity, individual data are shown only for the highest concentration (black symbols for WT and gray symbols for *Dcc*^{+/-}). Dashed inner circles represent a Rayleigh value of 0.5. **D–F**, Boxplots of the Rayleigh score at three NMDA concentrations between left and right L2 (**D**), left and right L5 (**E**), and between homolateral L2 and L5 (**F**). rL2 = right L2 ventral root; IL2 = left L2 ventral root; rL5 = right L5 ventral root; IL5 = left L5 ventral root (for statistics, see Extended Data Table 11-1).

studies using a spontaneous mutation allele that removes the exon encoding the P3 intracellular domain of DCC have shown that homozygous *Dcc*^{kanga/kanga} and *Dcc*^{kanga/-} mice exhibit a hopping gait, ataxia, and

abnormal pyramidal decussation through adulthood, thus recapitulating to some extent the motor phenotype of *DCC* haploinsufficient individuals (Finger et al., 2002; Welniarz et al., 2017). We therefore examined *Dcc*

heterozygous mice and assessed the contribution of *Dcc* to skilled motor and locomotor control, which relies on the integrity of the motor cortex and its corticospinal tract (Pourchet et al., 2021). We found that *Dcc*^{+/-} mice exhibited normal asymmetrical control of the forelimb during vertical exploration in the cylinder test; they also exhibited normal skilled forelimb coordination during voluntary locomotor control while walking on a wide and narrow beam and while crossing a horizontal ladder. Moreover, ICMS applied within cortical representations of the forelimb versus hindlimb evoked specific motor responses in forelimb or hindlimb muscles, respectively, in the *Dcc*^{+/-} mice, thus supporting the hypothesis that cortical areas and their corticospinal projections maintain their specificity. The absence of differences in cortical representations and the absence of differences in synaptic connectivity or latency of the corticospinal tract axons to the spinal cord in *Dcc*^{+/-} mice argue that cortical representation and functional connectivity of the corticospinal tract are normal in *Dcc*^{+/-} mice.

Increased duration of the duty cycle of the stance phase of adult *Dcc*^{+/-} mice during treadmill locomotion

In contrast to the hopping gait of *Dcc*^{kanga/kanga} and *Dcc*^{kanga/-} mutant mice (Finger et al., 2002; Welniarz et al., 2017) or conditional ablation of *Dcc* in *HoxB8*-expressing spinal neurons (Peng et al., 2018), we found no defects in locomotor gait of adult *Dcc*^{+/-} mice during treadmill locomotion. Although we only assessed *Dcc*^{+/-} mice at slow and intermediate walking speeds, no events of hop or gallop were observed during brief locomotor accelerations when the animals sped up to reach a locomotor frequency of 5–6 Hz. Among our locomotor data, the duty cycle of the stance phase was significantly increased in *Dcc*^{+/-} mice, especially at slow walking speed. Given the absence of changes in the duration of flexor and extensor-related locomotor activities and in their coupling during locomotor-like activity even at high NMDA concentrations using isolated spinal cord preparations, the increased duration of the duty cycle of the stance phase of *Dcc*^{+/-} mice might reflect a sensory feedback deficit. In support to this idea, *Netrin-1/Dcc* signaling guides sensory axons (Lakhina et al., 2012; Laumonnerie et al., 2014); *Netrin-1* and *Dcc*^{-/-} spinal cords exhibit an aberrant projection of cutaneous and proprioceptive axons in the spinal cord (Watanabe et al., 2006; Masuda et al., 2008; Laumonnerie et al., 2014) and *Dcc* is required for the normal development of nociceptive processing in mice and humans (da Silva et al., 2018). Furthermore, removing sensory afferents of semi-intact spinal cord preparations shortens the duration of the extensor phase during locomotion (Juvin et al., 2007); therefore, an aberrant sensory feedback in *Dcc*^{-/-} mice could presumably increase the duty cycle of their stance phase. Further studies will be necessary to test this hypothesis in mice and humans with the heterozygous mutation.

Spinal locomotor circuits are normal but show increased motoneuronal output modulation in neonatal *Dcc*^{+/-} mice

Using spinal cords isolated from neonatal mice, we also investigated the spinal locomotor circuit in the absence of

descending input from the brain and sensory feedback from the periphery. In contrast to *Dcc*^{-/-} or *Dcc*^{kanga/kanga} spinal cords (Rabe Bernhardt et al., 2012), those with *Dcc*^{+/-} mutation had normal coordination between left and right and between flexor-related and extensor-related motoneuronal output modulation during neonatal locomotion. Moreover, there were no significant differences in locomotor pattern and rhythm regardless of NMDA concentrations. However, the amplitude of the flexor-related motoneuronal activity was significantly increased in *Dcc*^{+/-} spinal cords on bath application of NMDA, suggesting that DCC plays a role in the establishment of the neuronal circuit modulating the excitability of the spinal locomotor circuit. Nevertheless, this increased output in flexor-related motoneuronal activity did not persist through adulthood, suggesting that sensory feedback might readjust the motoneuronal output of adult mutant mice. Perhaps comparative EMG studies of stepping in newborn, adolescent, and adult humans carrying monoallelic *DCC* mutations would reveal similar abnormalities during bipedal walking or quadrupedal crawling (Patrick et al., 2009; Vasudevan et al., 2016).

In summary, our study finds that, in contrast to humans, a heterozygous mutation in *Dcc* has little effect on skilled and basic locomotor control, or on the normal functioning of the motor cortex and its corticospinal connectivity. Although no functional impairments were found either in locomotor pattern and rhythm of spinal cord preparations isolated from neonatal mice, the flexor-related motoneuronal output was significantly increased in the developing spinal cord of *Dcc*^{+/-} mice. However, this increase in flexor-related motoneuronal output did not persist through adulthood and locomotor gait was overall normal, albeit with a longer duty cycle and less out-of-phase walk. This finding raises the possibility of the existence of subtle locomotor changes in humans carrying monoallelic *DCC* mutations.

References

- Bellardita C, Kiehn O (2015) Phenotypic characterization of speed-associated gait changes in mice reveals modular organization of locomotor networks. *Curr Biol* 25:1426–1436.
- Bretzner F, Liu J, Currie E, Roskams AJ, Tetzlaff W (2008) Undesired effects of a combinatorial treatment for spinal cord injury—transplantation of olfactory ensheathing cells and BDNF infusion to the red nucleus. *Eur J Neurosci* 28:1795–1807.
- Bretzner F, Plemel JR, Liu J, Richter M, Roskams AJ, Tetzlaff W (2010) Combination of olfactory ensheathing cells with local versus systemic cAMP treatment after a cervical rubrospinal tract injury. *J Neurosci Res* 88:2833–2846.
- Cazalets JR, Sqalli-Houssaini Y, Clarac F (1992) Activation of the central pattern generators for locomotion by serotonin and excitatory amino acids in neonatal rat. *J Physiol* 455:187–204.
- da Silva RV, Johannssen HC, Wyss MT, Roome RB, Bourojeni FB, Stifani N, Marsh APL, Ryan MM, Lockhart PJ, Leventer RJ, Richards LJ, Rosenblatt B, Srour M, Weber B, Zeilhofer HU, Kania A (2018) DCC is required for the development of nociceptive topognosis in mice and humans. *Cell Rep* 22:1105–1114.
- Ding YQ, Kim JY, Xu YS, Rao Y, Chen ZF (2005) Ventral migration of early-born neurons requires *Dcc* and is essential for the projections of primary afferents in the spinal cord. *Development* 132:2047–2056.

- Dominici C, Moreno-Bravo JA, Puiggros SR, Rappeneau Q, Rama N, Vieugue P, Bernet A, Mehlen P, Chédotal A (2017) Floor-plate-derived netrin-1 is dispensable for commissural axon guidance. *Nature* 545:350–354.
- Drew T, Doucet S (1991) Application of circular statistics to the study of neuronal discharge during locomotion. *J Neurosci Methods* 38:171–181.
- Drew T, Jiang W, Kably B, Lavoie S (1996) Role of the motor cortex in the control of visually triggered gait modifications. *Can J Physiol Pharmacol* 74:426–442.
- Fazeli A, Dickinson SL, Hermiston ML, Tighe RV, Steen RG, Small CG, Stoeckli ET, Keino-Masu K, Masu M, Rayburn H, Simons J, Bronson RT, Gordon JL, Tessier-Lavigne M, Weinberg RA (1997) Phenotype of mice lacking functional deleted in colorectal cancer (Dcc) gene. *Nature* 386:796–804.
- Finger JH, Bronson RT, Harris B, Johnson K, Przyborski SA, Ackerman SL (2002) The netrin 1 receptors *Unc5h3* and *Dcc* are necessary at multiple choice points for the guidance of corticospinal tract axons. *J Neurosci* 22:10346–10356.
- Fleming SM, Ekhtor OR, Ghisays V (2013) Assessment of sensorimotor function in mouse models of Parkinson's disease. *J Vis Exp* (76):50303.
- Flores C, Manitt C, Rodaros D, Thompson KM, Rajabi H, Luk KC, Tritsch NX, Sadikot AF, Stewart J, Kennedy TE (2005) Netrin receptor deficient mice exhibit functional reorganization of dopaminergic systems and do not sensitize to amphetamine. *Mol Psychiatry* 10:606–612.
- Friel KM, Drew T, Martin JH (2007) Differential activity-dependent development of corticospinal control of movement and final limb position during visually guided locomotion. *J Neurophysiol* 97:3396–3406.
- Izzi L, Charron F (2011) Midline axon guidance and human genetic disorders. *Clin Genet* 80:226–234.
- Jain RA, Bell H, Lim A, Chien CB, Granato M (2014) Mirror movement-like defects in startle behavior of zebrafish *dcc* mutants are caused by aberrant midline guidance of identified descending hindbrain neurons. *J Neurosci* 34:2898–2909.
- Jiang Z, Carlin KP, Brownstone RM (1999) An in vitro functionally mature mouse spinal cord preparation for the study of spinal motor networks. *Brain Res* 816:493–499.
- Juvin L, Simmers J, Morin D (2007) Locomotor rhythmogenesis in the isolated rat spinal cord: a phase-coupled set of symmetrical flexion extension oscillators. *J Physiol* 583:115–128.
- Keino-Masu K, Masu M, Hinck L, Leonardo ED, Chan SS, Culotti JG, Tessier-Lavigne M (1996) Deleted in colorectal cancer (DCC) encodes a netrin receptor. *Cell* 87:175–185.
- Kjaerulf O, Kiehn O (1996) Distribution of networks generating and coordinating locomotor activity in the neonatal rat spinal cord in vitro: a lesion study. *J Neurosci* 16:5777–5794.
- Kudo N, Yamada T (1987) N-methyl-D,L-aspartate-induced locomotor activity in a spinal cord-hindlimb muscles preparation of the newborn rat studied in vitro. *Neurosci Lett* 75:43–48.
- Kullander K, Butt SJ, Leuret JM, Lundfald L, Restrepo CE, Rydström A, Klein R, Kiehn O (2003) Role of EphA4 and EphrinB3 in local neuronal circuits that control walking. *Science* 299:1889–1892.
- Laflamme OD, Lemieux M, Thiry L, Bretzner F (2019) DSCAM mutation impairs motor cortex network dynamic and voluntary motor functions. *Cereb Cortex* 29:2313–2330.
- Lakhina V, Marcaccio CL, Shao X, Lush ME, Jain RA, Fujimoto E, Bonkowsky JL, Granato M, Raper JA (2012) Netrin/DCC signaling guides olfactory sensory axons to their correct location in the olfactory bulb. *J Neurosci* 32:4440–4456.
- Langlois SD, Morin S, Yam PT, Charron F (2010) Dissection and culture of commissural neurons from embryonic spinal cord. *J Vis Exp* (73):1773.
- Laumonerie C, Da Silva RV, Kania A, Wilson SI (2014) Netrin 1 and *Dcc* signalling are required for confinement of central axons within the central nervous system. *Development* 141:594–603.
- Lemieux M, Bretzner F (2019) Glutamatergic neurons of the gigantocellular reticular nucleus shape locomotor pattern and rhythm in the freely behaving mouse. *PLoS Biol* 17:e2003880.
- Lemieux M, Josset N, Roussel M, Couraud S, Bretzner F (2016) Speed-dependent modulation of the locomotor behavior in adult mice reveals attractor and transitional gaits. *Front Neurosci* 10:42.
- Liang DY, Zheng M, Sun Y, Sahbaie P, Low SA, Peltz G, Scherrer G, Flores C, Clark JD (2014) The Netrin-1 receptor DCC is a regulator of maladaptive responses to chronic morphine administration. *BMC Genomics* 15:345.
- Luong TN, Carlisle HJ, Southwell A, Patterson PH (2011) Assessment of motor balance and coordination in mice using the balance beam. *J Vis Exp* (49):2376.
- Masuda T, Watanabe K, Sakuma C, Ikenaka K, Ono K, Yaginuma H (2008) Netrin-1 acts as a repulsive guidance cue for sensory axonal projections toward the spinal cord. *J Neurosci* 28:10380–10385.
- Méneret A, Franz EA, Trouillard O, Oliver TC, Zagar Y, Robertson SP, Welniarz Q, Gardner RJM, Gallea C, Srour M, Depienne C, Jasoni CL, Dubacq C, Riant F, Lamy JC, Morel MP, Guérois R, Andreani J, Fouquet C, Doulazmi M, et al. (2017) Mutations in the netrin-1 gene cause congenital mirror movements. *J Clin Invest* 127:3923–3936.
- Metz GA, Whishaw IQ (2002) Cortical and subcortical lesions impair skilled walking in the ladder rung walking test: a new task to evaluate fore- and hindlimb stepping, placing, and co-ordination. *J Neurosci Methods* 115:169–179.
- Patrick SK, Noah JA, Yang JF (2009) Interlimb coordination in human crawling reveals similarities in development and neural control with quadrupeds. *J Neurophysiol* 101:603–613.
- Peng J, Charron F (2013) Lateralization of motor control in the human nervous system: genetics of mirror movements. *Curr Opin Neurobiol* 23:109–118.
- Peng J, Ferent J, Li Q, Liu M, Da Silva RV, Zeilhofer HU, Kania A, Zhang Y, Charron F (2018) Loss of *Dcc* in the spinal cord is sufficient to cause a deficit in lateralized motor control and the switch to a hopping gait. *Dev Dyn* 247:620–629.
- Pourchet O, Morel MP, Welniarz Q, Sarrazin N, Marti F, Heck N, Galléa C, Doulazmi M, Roig Puiggros S, Moreno-Bravo JA, Vidailhet M, Trembleau A, Faure P, Chédotal A, Roze E, Dusart I (2021) Loss of floor plate Netrin-1 impairs midline crossing of corticospinal axons and leads to mirror movements. *Cell Rep* 34:108654.
- Rabe N, Gezelius H, Vallstedt A, Memic F, Kullander K (2009) Netrin-1-dependent spinal interneuron subtypes are required for the formation of left-right alternating locomotor circuitry. *J Neurosci* 29:15642–15649.
- Rabe Bernhardt N, Memic F, Gezelius H, Thiebes AL, Vallstedt A, Kullander K (2012) DCC mediated axon guidance of spinal interneurons is essential for normal locomotor central pattern generator function. *Dev Biol* 366:279–289.
- Ritter LK, Tresch MC, Heckman CJ, Manuel M, Tysseling VM (2014) Characterization of motor units in behaving adult mice shows a wide primary range. *J Neurophysiol* 112:543–551.
- Schott GD, Wyke MA (1981) Congenital mirror movements. *J Neurol Neurosurg Psychiatry* 44:586–599.
- Serradj N, Paixão S, Sobocki T, Feinberg M, Klein R, Kullander K, Martin JH (2014) EphA4-mediated ipsilateral corticospinal tract misprojections are necessary for bilateral voluntary movements but not bilateral stereotypic locomotion. *J Neurosci* 34:5211–5221.
- Soblosky JS, Song JH, Dinh DH (2001) Graded unilateral cervical spinal cord injury in the rat: evaluation of forelimb recovery and histological effects. *Behav Brain Res* 119:1–13.
- Sparling JS, Bretzner F, Biernaskie J, Assinck P, Jiang Y, Arisato H, Plunet WT, Borisoff J, Liu J, Miller FD, Tetzlaff W (2015) Schwann cells generated from neonatal skin-derived precursors or neonatal peripheral nerve improve functional recovery after acute transplantation into the partially injured cervical spinal cord of the rat. *J Neurosci* 35:6714–6730.

- Srivatsa S, Parthasarathy S, Britanova O, Bormuth I, Donahoo AL, Ackerman SL, Richards LJ, Tarabykin V (2014) *Unc5C* and *DCC* act downstream of *Ctip2* and *Satb2* and contribute to corpus callosum formation. *Nat Commun* 5:3708.
- Srour M, Rivière JB, Pham JMT, Dubé MP, Girard S, Morin S, Dion PA, Asselin G, Rochefort D, Hince P, Diab S, Sharafaddinzadeh N, Chouinard S, Théoret H, Charron F, Rouleau GA (2010) Mutations in *DCC* cause congenital mirror movements. *Science* 328:592.
- Talpalar AE, Bouvier J, Borgius L, Fortin G, Pierani A, Kiehn O (2013) Dual-mode operation of neuronal networks involved in left-right alternation. *Nature* 500:85–88.
- Thiry L, Lemieux M, D Laflamme O, Bretzner F (2016) Role of *DSCAM* in the development of the spinal locomotor and sensorimotor circuits. *J Neurophysiol* 115:1338–1354.
- Varadarajan SG, Kong JH, Phan KD, Kao TJ, Panaitof SC, Cardin J, Eltzhig H, Kania A, Novitch BG, Butler SJ (2017) *Netrin1* produced by neural progenitors, not floor plate cells, is required for axon guidance in the spinal cord. *Neuron* 94:790–799.e3.
- Vasudevan EV, Patrick SK, Yang JF (2016) Gait transitions in human infants: coping with extremes of treadmill speed. *PLoS One* 11: e0148124.
- Watanabe K, Tamamaki N, Furuta T, Ackerman SL, Ikenaka K, Ono K (2006) Dorsally derived *netrin 1* provides an inhibitory cue and elaborates the ‘waiting period’ for primary sensory axons in the developing spinal cord. *Development* 133:1379–1387.
- Welniarz Q, Morel MP, Pourchet O, Gallea C, Lamy JC, Cincotta M, Doulazmi M, Belle M, Méneret A, Trouillard O, Ruiz M, Brochard V, Meunier S, Trembleau A, Vidailhet M, Chédotal A, Dusart I, Roze E (2017) Non cell-autonomous role of *DCC* in the guidance of the corticospinal tract at the midline. *Sci Rep* 7:410.
- Whishaw IQ (2000) Loss of the innate cortical engram for action patterns used in skilled reaching and the development of behavioral compensation following motor cortex lesions in the rat. *Neuropharmacology* 39:788–805.
- Zar JH (1996) *Biostatistical analysis*, Ed 3. Upper Saddle River: Prentice Hall Inc.
- Z’Graggen WJ, Metz GA, Kartje GL, Thallmair M, Schwab ME (1998) Functional recovery and enhanced corticofugal plasticity after unilateral pyramidal tract lesion and blockade of myelin-associated neurite growth inhibitors in adult rats. *J Neurosci* 18:4744–4757.
- Zhang Y, Narayan S, Geiman E, Lanuza GM, Velasquez T, Shanks B, Akay T, Dyck J, Pearson K, Gosgnach S, Fan CM, Goulding M (2008) *V3* spinal neurons establish a robust and balanced locomotor rhythm during walking. *Neuron* 60:84–96.